UNIVERSITY OF OKLAHOMA
GRADUATE COLLEGE

ASSESSING THE SKILL AND RELIABILITY OF NCAR-CESM SMYLE PREDICTIONS OF THE NORTH ATLANTIC SUBTROPICAL HIGH IN MULTI-YEAR TIMESCALES

A THESIS
SUBMITTED TO THE GRADUATE FACULTY
in partial fulfillment of the requirements for the
Degree of
MASTER OF SCIENCE

by GWYNETH L GLANTON
Norman, Oklahoma
2026

Downloaded from SHAREOK. Persistent Handle URL: https://hdl.handle.net/11244/343200

ASSESSING THE SKILL AND RELIABILITY OF NCAR-CESM SMYLE PREDICTIONS OF THE NORTH ATLANTIC SUBTROPICAL HIGH IN MULTI-YEAR TIMESCALES

A THESIS APPROVED FOR THE
SCHOOL OF METEOROLOGY

BY THE COMMITTEE CONSISTING OF

Dr. Kathleen Pegion (Chair)

Dr. Jason Furtado

Dr. Emily Becker

©Copyright by GWYNETH L GLANTON 2026

All Rights Reserved.

Acknowledgments

They say it is the people who make a place, and I feel incredibly fortunate to have been surrounded by amazing colleagues, professors, scientists, and friends throughout my time at the University of Oklahoma. The University of Oklahoma has been my home for the past six years, and the people I have met along the way are what made this place so special to me.

First, I want to thank my advisor, Dr. Kathy Pegion, who took a chance on me my senior year and guided me through this research. I would not have made it through this process without her support, guidance, and encouragement. I would also like to thank my committee members, Dr. Jason Furtado and Dr. Emily Becker, for their advice and support throughout the thesis process. Additionally, I would like to thank the School of Meteorology staff and all of the professors who guided me toward this goal. Their patience, knowledge, and support are deeply appreciated. Specifically, I want to give a huge shout-out to Dr. Harold Brooks, who provided invaluable advice and knowledge that helped me through my last semester. I will forever appreciate the mentors, connections, and opportunities that have shaped me into the scientist I am today.

Lastly, I would like to thank my parents, friends, and my dog, Honey Bee. Without my parents, I would not be the woman or person I am today. Their unwavering support and encouragement to follow my dreams allowed me to thrive and grow to my full potential. Thank you for everything you do. To the friends and connections I have made here, I would not have gotten through this without you and will miss seeing you everyday. I would also like to dedicate a part of my journey to three of my friends who lost their lives in 2022: Drake, Nic, and Gavin. I know they are cheering me on from

above.

Thank you to everyone who has been a part of my journey, big or small. Oklahoma will always have a piece of my heart, and I will forever be a Sooner. Boomer!

Table of Contents

Acknowledgments iv

List of Tables viii

List of Figures ix

Abstract xiii

1 Introduction 1
- 1.1 Southeast United States Precipitation 2
- 1.2 Introducing The NASH 3
- 1.3 Subtropical Highs and the AMO 4
- 1.4 Current Understanding 5
- 1.5 Research Questions 6

2 Data and Methods 8
- 2.1 Datasets 8
  - 2.1.1 NCAR-CESM Seasonal to Multi-Year Large Ensemble Model . . 8
  - 2.1.2 Fifth-Generation ECMWF Atmospheric Reanalysis Data 9
  - 2.1.3 Climate Hazards Group InfraRed Precipitation with Station Data 10
- 2.2 Detection and Characterization of the NASH 10
  - 2.2.1 Western Ridge Detection 10
- 2.3 Precipitation Verification 11

3 Results 14
- 3.1 How Skillfully Does CESM2-SMYLE Predict the NASH Western Ridge? 14
  - 3.1.1 Why Is Bias Correction Necessary? 15
  - 3.1.2 How Accurately Does SMYLE Predict the NASH Western Ridge Position? 16
- 3.2 How Well Does SMYLE Predict Precipitation? 22
  - 3.2.1 Deterministic and Probabilistic Precipitation Performance . . . 22
- 3.3 Does Correct NASH Western Ridge Prediction Improve SEUS Precipitation Prediction? 28
  - 3.3.1 Does Correct NASH Prediction Improve Probabilistic Skill? . . 28

3.3.2 How Does Correct NASH Prediction Affect Precipitation Forecasts? . . . 29
3.4 What Limits Prediction Skill? . . . 35
3.4.1 Errors Despite Correct Circulation . . . 37

4 Discussion and Conclusions . . . 43
4.0.1 Discussion . . . 43
4.1 What Have We Learned About NASH Western Ridge Prediction Skill? 43
4.2 What Have We Learned About Precipitation Prediction Skill? . . . 45
4.3 Why Does Correct NASH Prediction Not Guarantee Correct Precipitation? . . . 47
4.4 Broader Implications . . . 48
4.5 Limitations . . . 49
4.6 Future Work . . . 50
4.6.1 Summary and Conclusion . . . 51

Reference List . . . 52

List of Tables

List of Figures

1.1 NASH westward extension over the SEUS region to show how the western ridge could influence increased rainfall in the region. Two lines represent a weak NASH (blue) and a strong NASH (orange) and the corresponding moisture transport direction. Figure from Zhang et al. (2022). 7

3.1 Comparison of the NASH western ridge positions and the climatological NASH western ridge position in raw SMYLE (black X), ERA5 (yellow cross), and bias-corrected SMYLE (orange star). Three leads are shown for the initialization of May over a map of the North Atlantic Ocean. . 16

3.2 Not bias-corrected latitude (N-S)(a) and longitude (E-W)(b) distance errors for 4 initialization times (February, May, August, and November). Lead time is on the x-axis in months, and the difference (SMYLE - ERA5) in degrees is on the y-axis. The mean position error for each lead time is shown with a colored diamond, the median with a black line, and the range of ensemble difference errors (box plots). This is calculated across the years 1970-2019 and for all 20 ensembles. 17

3.3 Bias-corrected latitude (N-S)(a) and longitude (E-W)(b) distance errors for 4 initialization times (February, May, August, and November). Lead time is on the x-axis in months, and the difference (SMYLE - ERA5) in degrees is on the y-axis. The mean position error for each lead time is shown with a colored diamond, the median with a black line, and the range of ensemble difference errors (box plots). This is calculated across the years 1970-2019 and for all 20 ensembles. 18

3.4 Percentage of correctly predicted NASH western ridge quadrants as a function of forecast initialization and lead time. A prediction is classified as correct when the SMYLE western ridge occurs in the same climatologically defined quadrant as the corresponding ERA5 western ridge. Shading indicates the percentage of forecasts with matching SMYLE and ERA5 quadrant classifications. 20

3.5 Percentage of correctly predicted NASH western ridge quadrants during the first June-August period following each SMYLE initialization. Panels correspond to the northwest (NW), northeast (NE), southwest (SW), and southeast (SE) quadrants. 21

3.6 Brier Score (BS) for probabilistic SMYLE forecasts of above-average precipitation as a function of lead time for each initialization. The respective solid color line represents the SMYLE ensemble Brier score and the gray dashed line represents the CHIRPS climatology Brier score. . . 24

3.7 Brier Skill Score (BSS) for probabilistic SMYLE forecasts of above-average precipitation as a function of lead time for each initialization. The BSS reference forecast is the observed CHIRPS climatological probability of above-average precipitation for each calendar month and grid point. Positive BSS values indicate skill relative to climatology, whereas negative values indicate lower skill than climatology. 25

3.8 Reliability diagram for selected lead times of SMYLE probabilistic forecasts of above-average precipitation. Forecast probabilities are compared with the observed frequency of above-average precipitation from CHIRPS. Green shading represents underforecasting the probability, and red represents overcasting the probability. The one-to-one line represents perfect reliability. 26

3.9 Area under the receiver operating characteristic curve (ROC AUC) for pooled SMYLE forecasts of above-average precipitation as a function of forecast lead for each initialization. An AUC of 0.5 indicates no discrimination between above-average and below-average precipitation events, while values greater than 0.5 indicate increasing discriminatory ability. 27

3.10 Brier Score for above-average precipitation forecasts conditioned on correct (solid green line) and incorrect prediction (dashed orange line) of the NASH western ridge quadrant for the 4 initializations by lead time (month, x-axis). Results are compared with the corresponding full-ensemble precipitation forecast. CHIRPS climatology (dotted gray line) and all members (solid black line) are present for comparison. 30

3.11 Brier Score difference for above-average precipitation forecasts conditioned on correct prediction of the NASH western ridge quadrant and an equally sized random subset of the full ensemble for the 4 initializations by lead time (month, x-axis). Negative areas are shaded blue to show NASH conditioning improves BS, and the positive difference is shaded in orange to show that no added value occurred from NASH conditioning. Leads with fewer than 10 matched years are annotated. . 31

3.12 Agreement between SMYLE and CHIRPS precipitation categories when the NASH western ridge quadrant is correctly (solid green line) and incorrectly (dashed orange line) predicted in percentages per lead time(months). The 4 initializations are represented in the panels. Gray annotations indicate the number of member-level samples used for the NASH-correct and NASH-incorrect groups, respectively (correct/incorrect). 34

3.13 Spatial distribution of precipitation forecast performance conditioned on the accuracy of the predicted NASH western ridge quadrant. The 4 initializations are represented in the panels, and positive values (blue) indicate greater precipitation accuracy among NASH-correct members. 35

3.14 Reliability of probabilistic above-average precipitation forecasts conditioned on correct (solid green line) and incorrect (dashed orange line) NASH western ridge prediction. Forecast probabilities are compared with the observed frequency of above-average precipitation from CHIRPS. 36

3.15 Receiver operating characteristic (ROC) curves for precipitation forecasts conditioned on correct (solid green line) and incorrect (dashed orange line) prediction of the NASH western ridge quadrant per lead time (months). The area under each curve summarizes the ability of each forecast subset to discriminate between above-average and below-average precipitation events. 37

3.16 May initialization first-summer circulation and precipitation errors by NASH western-ridge position error. SMYLE 850 hPa bias-corrected (black line) and ERA5 850 hPa (dashed green line), precipitation anomaly differences (colorbar, mm/day), mean SMYLE western ridge position (blue X), and mean ERA5 western ridge location (orange cross) for forecasts separated by NASH western ridge point distance error bin (poor, moderate, good, and excellent). 41

3.17 May initialization first summer circulation and precipitation error by NASH western-ridge longitude error. SMYLE 850 hPa bias-corrected (black line) and ERA5 850 hPa (dashed green line), precipitation anomaly differences (colorbar, mm/day), mean SMYLE western ridge position (blue X), and mean ERA5 western ridge location (orange cross) for forecasts separated by NASH western ridge point longitude-error bin (too far west, near longitude, too far east) 42

3.18 May initialization first-summer circulation and precipitation errors by NASH quadrant prediction skill. SMYLE 850 hPa bias-corrected (black line) and ERA5 850 hPa (dashed green line), precipitation anomaly differences (colorbar, mm/day), mean SMYLE western ridge position (blue X), and mean ERA5 western ridge location (orange cross) for forecasts separated by NASH western ridge quadrant prediction. 42

Abstract

The North Atlantic Subtropical High (NASH), also known as the Bermuda High, is a semi-permanent high-pressure system located over the North Atlantic Ocean that influences summertime climate across the southeastern United States (SEUS). Variations in the strength and position of the NASH western ridge affect regional circulation and are associated with changes in precipitation, heat, drought, and coastal inundation. Since low-frequency sea surface temperature variability may contribute to variations in NASH position, initialized climate predictions could provide a source of multi-year (1-2 years) predictability for the NASH and its regional impacts.

This study evaluates the ability of the NCAR Community Earth System Model Seasonal-to-Multiyear Large Ensemble (SMYLE) hindcasts to predict the NASH western ridge and associated SEUS precipitation at lead times extending to two years. SMYLE western-ridge positions are evaluated against ERA5 reanalysis, and precipitation forecasts are verified against CHIRPS observations. Systematic biases in the simulated NASH are addressed before evaluating western-ridge position and quadrant prediction. Precipitation prediction is assessed using probabilistic verification metrics, including the Brier Score, Brier Skill Score, and receiver operating characteristic area under the curve (ROC AUC). Precipitation skill is additionally conditioned on whether individual ensemble members correctly predict the observed NASH quadrant to determine whether improved representation of the NASH is associated with improved precipitation prediction.

SMYLE exhibits a systematic bias in the NASH western ridge position, particularly in longitude, and removing the mean bias improves agreement with ERA5. Considerable case-to-case variability in western-ridge position remains after bias correction, and

quadrant prediction varies with initialization, lead time, season, and observed NASH quadrant. SEUS precipitation forecasts exhibit limited skill relative to climatology, although SMYLE retains some ability to discriminate between above- and below-average precipitation conditions. Conditioning the forecasts on correct NASH quadrant prediction generally improves precipitation prediction relative to members that incorrectly predict the NASH, but these improvements do not consistently result in greater skill than climatology or the full ensemble. Circulation composites further show that correct quadrant classification does not necessarily correspond to an exact representation of the NASH western ridge or regional precipitation. In particular, the direction of longitudinal western-ridge errors is associated with systematic precipitation differences, with eastward ridge errors generally corresponding to wetter SMYLE conditions and westward errors to drier conditions.

These results demonstrate that accurate prediction of the NASH provides some useful information for SEUS precipitation prediction, but NASH quadrant prediction alone is insufficient to determine precipitation skill in this region. The results highlight both the potential value of the NASH as a source of multi-year regional climate predictability and the importance of representing the position of the western ridge when translating circulation predictability into regional precipitation forecasts.

Chapter 1

Introduction

Precipitation fluctuations in a region can have a major influence on regional hydrology, agriculture, and other related industries. The interannual variability of summer precipitation in the Southeast United States (SEUS) has increased significantly in recent decades, posing a threat to the region's water supply (Li et al., 2012a; Schmidt and Grise, 2019; Wang et al., 2010). The increase in both drought and heavy precipitation events has been shown to alter runoff, increase soil erosion, and affect crop yields. Several studies have evaluated the factors influencing precipitation variability in this region, emphasizing atmospheric circulation anomalies (Li et al., 2012a, 2013; Wei et al., 2019). While tropical drivers like the El Niño Southern Oscillation (ENSO) explain some of the variability, especially in winter, summer rainfall remains less predictable (Pegion et al., 2022; Schubert et al., 2009). A significant contributor to summer precipitation in the SEUS is the North Atlantic Subtropical High (NASH), a semi-permanent system located over the North Atlantic Ocean in the lower troposphere (Davis et al., 1997; Li et al., 2011; Zorzetto and Li, 2021; Schmidt and Grise, 2019). However, it remains unclear whether initialized climate prediction systems can accurately predict NASH variability and whether that skill translates into improved forecasts of summertime precipitation. This study aims to investigate the interplay between NASH variability and the predictability of precipitation in the SEUS.

1.1 Southeast United States Precipitation

SEUS precipitation variability arises from a combination of factors, including remote forcing, local factors, sea surface temperature (SST) anomalies, and climate variability. Remote forcing, particularly ENSO, has a strong influence on SEUS hydroclimate on a multi-year timescale during winter months when teleconnections are most robust (Misra et al., 2018; Smith and Sheridan, 2022). During La Niña years, winters are dry in the SEUS, while El Niño winters are typically wetter. However, these relationships weaken during the summer, when tropical-extratropical interactions are less direct (Branstator, 2002; Schubert et al., 2011; Di Capua et al., 2020). These teleconnections can align with the Mid-Latitude Seasonal Oscillation (MLSO) on a seasonal timescale, which can influence winter precipitation through the westerlies. In a positive MLSO phase, the westerlies are much stronger and enhance baroclinic activity, often bringing below-average temperatures and increased precipitation. In the negative phase, westerlies are weakened and reduce frontal activity, leading to warmer and drier conditions (Manthos et al., 2022). On a subseasonal timescale, the Madden–Julian Oscillation (MJO) can further influence SEUS hydroclimate by modulating the intensity and position of midlatitude jets, which affects cold-season precipitation events (Zhou et al., 2021; Becker et al., 2011). In contrast, local and regional processes such as soil moisture variability, diurnal convection, and land–atmosphere coupling play an important role in warm-season precipitation variability. These processes form feedback loops that regulate surface heat fluxes, cloud formation, atmospheric heat and moisture, and ultimately modulate convection and precipitation intensity (Ek and Holtslag, 2005; Li et al., 2013; Cioni and Hohenegger, 2017; Ford et al., 2023). During this season, the land–sea contrast largely drives the NASH, particularly the westward extension, which shapes prevailing moisture transport as seen in 1.1 (Hoskins, 1996; Rodwell and

Hoskins, 2001; Li et al., 2011; Schmidt and Grise, 2019).

1.2 Introducing The NASH

NASH's changes in strength and position affect U.S. summer precipitation, especially in the SEUS. When considering summer precipitation on different timescales, the NASH plays an important role in moisture transport and vertical motion (Zhang et al., 2022). This is especially true for the western ridge of the NASH, which has been known to influence rainfall during boreal summers (Li et al., 2012a, 2013; Wei et al., 2019; Nigam et al., 2011). The NASH's western ridge can be characterized into four quadrants based on the location from its climatological center: northeast (NE), northwest (NW), southeast (SE), and southwest (SW). The precipitation response associated with the western ridge depends strongly on its position relative to climatology. Northwestward displacement is generally associated with hotter and drier conditions over portions of the United States, whereas southwestward displacement can enhance low-level moisture transport into the SEUS and favor wetter conditions (Li et al., 2011, 2012a,b, 2013, 2019; Nigam et al., 2011; Wei et al., 2019). These relationships motivate the quadrant framework used later in this study. Thus, variations in the NASH can represent a connection between oceanic forcing and precipitation variability. North Atlantic SST anomalies also play a crucial role in modulating SEUS summer precipitation by influencing tropical cyclone activity and subtropical circulation patterns. Warmer SSTs in the tropical North Atlantic can influence the formation, intensity, and tracks of tropical cyclones, which can affect precipitation in the SEUS (Xu et al., 2016; Chalise et al., 2021; Liu et al., 2025). On multidecadal timescales, such variability can be tied to the Atlantic Multidecadal Oscillation (AMO), which influences these SST–circulation relationships through its impact on the NASH.

1.3 Subtropical Highs and the AMO

Subtropical highs are fundamental elements of atmospheric circulations that are most prevalent in boreal summer. Large-scale circulation features such as the NASH are influenced by multidecadal variations in North Atlantic sea surface temperatures, including the Atlantic Multidecadal Oscillation (AMO) (Hu et al., 2011). The AMO is defined as the North Atlantic SST anomalies on a basin scale (0°-60°N and 75°-7.5°W) for a 65-80 year cycle, exhibiting a positive (warm) phase and a negative (cold) phase (Kerr, 2000; Enfield et al., 2001). Several studies have found that during the AMO's warm phase, the NASH weakens, contracts, and shifts northeastward, diminishing its influence on the North American climate. This has been associated with drought, low precipitation, and higher temperatures in the SEUS (Enfield et al., 2001; Nigam et al., 2011; Alexander et al., 2014). The North Atlantic Ocean SST during this phase would be warmer than usual, allowing an air mass in the region of the high-pressure system to spread downstream, causing a decrease in air mass accumulation in the core region. This reduction leads to a lowering of sea level pressure (SLP), which in turn weakens the NASH and the associated low-level clockwise winds. Such weakening during summer months allows the enhancement of thermal low-pressure systems over the United States and enhances easterly flow into the SEUS (Hu et al., 2011). This weakened state is found to be related to an eastward retreat of the NASH's western ridge. Conversely, when the AMO is in the cold phase, the colder-than-average SSTS enhance the NASH and cause a significant westward shift of its climatological position, extending its influence over the SEUS (Hu et al., 2011; Li et al., 2011). This provides an understanding of NASH behavior and its influence on precipitation on the multidecadal timescale. Since the NASH has been shown to respond to North Atlantic SST variability, it is possible that some aspects of its variability may also exhibit predictability on a shorter

timescale. Initialized climate prediction systems provide a framework for evaluating this hypothesis by testing whether observed initial ocean and atmospheric conditions improve forecasts of NASH variability.

1.4 Current Understanding

Since the late 20th century, observational and reanalysis data show that the NASH has become more intense and westward-shifted (He et al., 2017; Li et al., 2012b, 2019; Song et al., 2018; Zhou et al., 2021). Climate projection studies using uninitialized models further suggest that these long-term changes may continue under future warming scenarios. For example, a study from Li et al. (2019) used different phases of the Coupled Model Intercomparison Project (CMIP) outputs under the historical (1950-1999) and the Representative Concentration Pathways 8.5 (RCP8.5) scenario (2050-2099) to evaluate this. This study found a significant increase in the number of NW-type and SW-type ridges, particularly in SW-type ridges. Whereas the amount of SE- and NE-type ridges will decrease significantly. These projected changes imply substantial shifts in summertime moisture transport and precipitation over the SEUS. While these studies improve our understanding of how the NASH may respond to long-term climate change, they do not address whether year-to-year or multi-year variations in the NASH are predictable. In particular, it remains unknown whether initialized prediction systems can skillfully predict the position and variability of the NASH western ridge and whether accurate prediction of the NASH can improve forecasts of summertime precipitation. Addressing these questions represents a critical step toward understanding the limits of warm-season hydroclimate predictability in the Southeast United States.

1.5 Research Questions

While multi-year and decadal variability of winter precipitation in SEUS has been extensively investigated, the mechanisms behind multi-year summer precipitation remain less well understood (Pegion et al., 2022; Manthos et al., 2022). As a result, substantial uncertainties persist in projecting the frequency, duration, and intensity of warm-season rainfall events. These uncertainties arise from the limited understanding associated with how large-scale climate modes interact with regional atmospheric dynamics to modulate moisture transport. In addition, current models struggle to quantify the land-atmosphere feedbacks and the circulation patterns that influence SEUS summer rainfall. Together, the physical processes linking climate variability modes to warm-season precipitation are still not fully resolved, underscoring the need to improve our understanding of warm-season predictions and the mechanisms of prediction. This study addresses these gaps by examining whether variability in the North Atlantic Subtropical High can serve as a source of multi-year predictability for summer precipitation in the SEUS. By investigating seasonal to two-year variations in the NASH, this work will improve our understanding of the mechanisms governing warm-season hydroclimate variability and help determine whether the NASH represents a useful source of multi-year predictability for the Southeast United States. This study aims to answer three main questions:

1. To what extent can initialized 2-year predictions skillfully represent the variability in the frequency and position of the North Atlantic Subtropical High?

2. How skillfully do initialized 2-year predictions predict summertime above- and below-average precipitation over the Southeast United States?

3. Does correct prediction of the NASH western ridge improve summertime precip-

itation prediction skill over the Southeast United States?

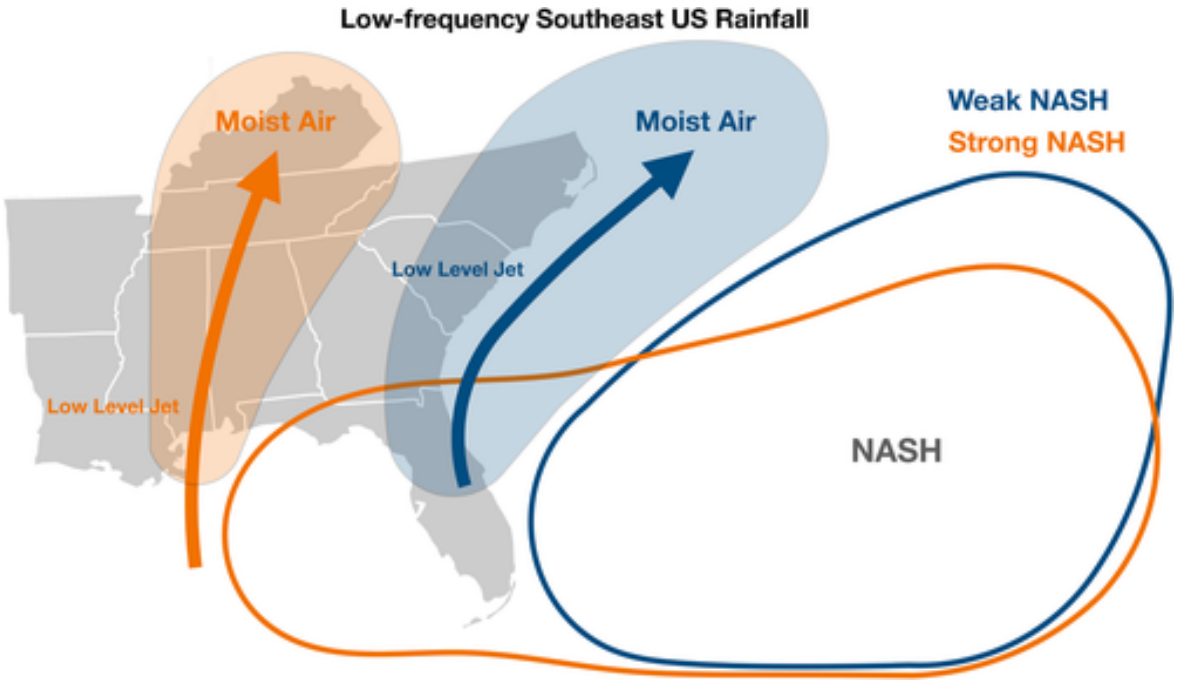


Figure 1.1: NASH westward extension over the SEUS region to show how the western ridge could influence increased rainfall in the region. Two lines represent a weak NASH (blue) and a strong NASH (orange) and the corresponding moisture transport direction. Figure from Zhang et al. (2022).

Chapter 2

Data and Methods

This research investigates the skill of the NASH and associated precipitation using model hindcasts. Model details, comparison data specifications, and analysis techniques are provided in this section. The analysis is structured to evaluate whether the model hindcasts can predict the variability of the NASH out to 2-year lead times and to assess whether this variability provides a pathway for summer precipitation prediction. First, the forecast skill of the NASH western ridge is evaluated as a function of lead time. Second, the relationship between NASH variability and precipitation is quantified using average precipitation classifications. Finally, precipitation skill is assessed conditional on correct NASH predictions to determine whether circulation predictability translates into precipitation prediction skill.

2.1 Datasets

2.1.1 NCAR-CESM Seasonal to Multi-Year Large Ensemble Model

Motivated by evidence that the NASH exhibits two-year variability influenced by oceanic forcing, initialized multi-year model simulations are used to evaluate the prediction of its spatial variability and associated characteristics. The initialized hindcast data used in this study are from the NCAR-CESM Seasonal to Multi-Year Large En-

semble (SMYLE) model (Yeager et al. 2022). The SMYLE hindcasts are initialized quarterly (1st of February, May, August, November) from 1970 to 2019, with 24-month runs using 20-member ensembles. This study will use the monthly outputs to evaluate the variability in the location of the NASH western ridge and the daily outputs averaged for each month for the precipitation study. The set uses CESM2 component models at a nominal 1-degree horizontal resolution for the atmosphere, ocean, land, sea ice, and ocean biogeochemistry. The atmospheric component of CESM2 is CAM6, the ocean component is POP2, the land component is CLM5, the sea ice component is CICE5, and the ocean biogeochemistry component is the MARBL. The atmosphere model CAM6 is initialized using JRA55 reanalysis data, the POP2 and CICE5 are initialized using the JRA55-do forced ocean/sea-ice (FOSI) simulation, and CLM5 is initialized using the CRU-JRAv2 forced land simulation.

To remove systematic model bias, monthly climatological geopotential height fields were computed separately for each initialization month and forecast lead using all ensemble members and years. SMYLE anomalies were calculated relative to these lead-dependent climatologies. The ERA5 monthly climatology was then added to the SMYLE anomalies to reconstruct bias-corrected geopotential height fields while preserving the observed climatological mean state for western ridge detection.

2.1.2 Fifth-Generation ECMWF Atmospheric Reanalysis Data

To verify the prediction of the NASH location, it is compared to the fifth-generation ECMWF atmospheric reanalysis data (ERA5) (Hersbach et al., 2023). ERA5 data provides hourly estimates of atmospheric, land, and oceanic climate variables that are averaged monthly. This study uses ERA5 data for the years that correspond with the SMYLE hindcasts, including the 24-month lead time that follows the final year of the SMYLE data (1970-2021). The data has a horizontal resolution of 0.25 degrees by 0.25

degrees on a regular lat-lon grid that is interpolated using bilinear interpolation to the SMYLE hindcast's horizontal resolution. ERA5 has a vertical resolution of 137 levels, and the 850 hPa level is used in this study.

2.1.3 Climate Hazards Group InfraRed Precipitation with Station Data

To verify precipitation predictions from SMYLE, the Climate Hazards Group Infrared Precipitation with Station (CHIRPS) data is used (Funk et al., 2015). CHIRPS is a quasi-global dataset with a spatial resolution of 0.25 degrees by 0.25 degrees that integrates satellite infrared observations with ground station networks. Daily CHIRPS precipitation was aggregated to monthly mean daily precipitation across the years 1981-2020. The dataset is regridded to the SMYLE hindcasts grid using the xESMF conservative normed method. This approach calculates precipitation on each SMYLE grid cell from the area-weighted contributions of overlapping CHIRPS grid cells while accounting for missing source-grid values.

2.2 Detection and Characterization of the NASH

2.2.1 Western Ridge Detection

To investigate the variability of the NASH in ERA5 and its potential impacts on SEUS precipitation, we define the location of the NASH western ridge based on Li et al. (2011) using the 850 hPa zonal winds and the 850 hPa geopotential height between 0°- 60°N and 120°-0°W. The latitude and longitude location of the western ridge for a given month is determined by finding the most westerly intersection between the 1560 gpm isoline and the wind line where the easterly component of U850 reverses to be westerly,

or where

$$u = 0$$

and

$$\frac{\partial u}{\partial y} > 0$$

. If no intersection is found, no NASH western ridge location is identified for that month. The climatological location of the western ridge for the SMYLE hindcasts is found for each lead time. Western ridge positions were classified into four quadrants relative to the lead-dependent climatological position following Li et al. (2011), as Northwest (NW), Northeast (NE), Southwest (SW), or Southeast (SE). The quadrant framework captures both meridional and zonal displacements simultaneously while reducing sensitivity to small positional errors and providing a physically meaningful classification for statistical analysis.

2.3 Precipitation Verification

For each forecast, a binary above- and below-average probability distribution is calculated from the SMYLE ensemble distribution and compared against the observed category from CHIRPS. Since above- and below-average precipitation are complementary binary events, verification is presented for above-average precipitation. Forecast discrimination was evaluated using the area under the receiver operating characteristic curve (ROC AUC), which summarizes the trade-off between the true positive rate and false positive rate across all probability thresholds.

Probabilistic precipitation forecasts are evaluated using the Brier score (BS)

$$BS = \frac{1}{N} \sum_{i=1}^{N} (p_i - o_i)^2 \tag{2.1}$$

where p_i is the forecast probability of above-average precipitation, o_i is the corresponding binary CHIRPS observation (0 or 1), and N is the number of forecast-observation pairs included in the verification. The Brier Score therefore represents the mean squared error of the forecast probabilities. A perfect probabilistic forecast has a BS of 0, while larger values indicate greater probability error. For each calendar month and grid point, the climatological probability of above-average precipitation was calculated from the frequency of observed above-average precipitation during the climatological period. This probability was then used as the forecast probability for the corresponding month and grid point when calculating $BS_{\text{climatology}}$. Thus, the climatology line shown in the Brier Score figures represents the Brier Score that would be obtained by issuing the observed climatological probability of above-average precipitation rather than using the SMYLE forecast probabilities.

Forecast skill relative to climatology is evaluated using the Brier Skill Score (BSS),

$$BSS = 1 - \frac{BS_{\text{forecast}}}{BS_{\text{climatology}}} \tag{2.2}$$

.

where BS_{forecast} is the Brier Score of the SMYLE forecast and $BS_{\text{climatology}}$ is the Brier Score obtained using the observed CHIRPS climatological probability of above-average precipitation as the reference forecast. The climatological probability is calculated separately for each calendar month and grid point so that the reference forecast retains the observed seasonal and spatial variability in the frequency of above-average precipitation. A BSS greater than 0 indicates that SMYLE outperforms the climatological probability forecast, a BSS of 0 indicates equivalent performance, and a negative BSS indicates poorer performance than climatology.

When conditioning precipitation on correct NASH western ridge predictions and

comparing to unconditioned precipitation skill, ensemble-size matching was used. Since the number of NASH-correct and NASH-incorrect members varies among years and lead times, the two groups are matched to a common ensemble size, $k = min(n_{correct}, n_{incorrect})$. Years with fewer than three members in either group are excluded from the conditional analysis. To control for differences in the verification sample, all forecasts within the conditional comparison are evaluated over the same retained, or paired, years. The full 20-member ensemble and climatological reference are therefore recalculated over these same years.

Finally, an expected Brier Score for an equally sized random k-member subset of the full ensemble is calculated to determine whether differences associated with NASH-correct member selection exceed those expected from ensemble-size effects alone. This ensures that differences in forecast skill reflect NASH western ridge location prediction rather than differences in sample size.

Chapter 3

Results

This chapter addresses the three research questions posed in Chapter 1. First, the ability of SMYLE to predict the NASH western ridge is investigated, including the influence of systematic model bias and the accuracy of the predicted ridge position. Second, the deterministic and probabilistic skill of SMYLE precipitation forecasts is assessed. Finally, precipitation forecast performance is investigated conditional on the accuracy of the predicted NASH western ridge to determine whether improved circulation prediction relates to improved precipitation prediction. Remaining forecast errors are then examined to identify factors that may limit precipitation prediction skill.

3.1 How Skillfully Does CESM2-SMYLE Predict the NASH Western Ridge?

This section addresses the first research question by evaluating whether SMYLE can reproduce the observed position and variability of the NASH western ridge. The influence of systematic model bias is first examined before prediction accuracy is investigated using ridge-position errors and categorical quadrant agreement.

3.1.1 Why Is Bias Correction Necessary?

Before evaluating prediction skill, systematic differences between SMYLE and ERA5 circulation are identified. Raw SMYLE western ridge positions exhibit positional biases relative to ERA5, particularly in the westward direction. The following analyses evaluate the magnitude, seasonality, and spatial structure of these biases and determine how bias correction aids in the predicted NASH western ridge.

Evaluation of the raw SMYLE hindcasts reveals a systematic bias in the predicted NASH western ridge position relative to ERA5. As shown in Figure 3.1, the non-bias-corrected SMYLE climatological ridge position is displaced westward of the ERA5 climatological position for all three leads shown for the May initialization. This behavior is also evident across all initializations and lead times in Figure 3.2. Longitude position errors, defined as the SMYLE minus ERA5 western ridge longitude, are predominantly negative, indicating a persistent westward displacement of the western ridge. The largest zonal biases occur during fall and winter, when mean longitude errors approach 30° in magnitude for several lead times. In contrast, late spring and summer exhibit smaller longitude errors, with mean values closer to 0°. Latitude position errors are substantially smaller than longitude errors, with mean positional errors being under plus-or-minus 5° across all leads. Latitude errors show a tendency toward a northward displacement during summer and a southward displacement during winter. Together, these results indicate that systematic error in the raw SMYLE western ridge position is dominated by east-west displacement, with a seasonal dependence. Therefore, raw ridge locations cannot be fairly compared with ERA5 because of the systematic positional biases and need to be corrected.

Following bias correction, the SMYLE climatological western ridge position shifts closer to the corresponding ERA5 climatological position, as illustrated in Figure 3.1.

Additionally, in Figure 3.3, the mean latitude and longitude position errors are also reduced toward 0° across forecast leads and initialization times. The reduction is particularly evident in the east-west direction, where the strong westward displacement present in the raw hindcasts is substantially diminished. Bias correction therefore reduces the systematic differences between the SMYLE and ERA5 mean states, allowing the analyses to focus on forecast variability and prediction error rather than model bias.

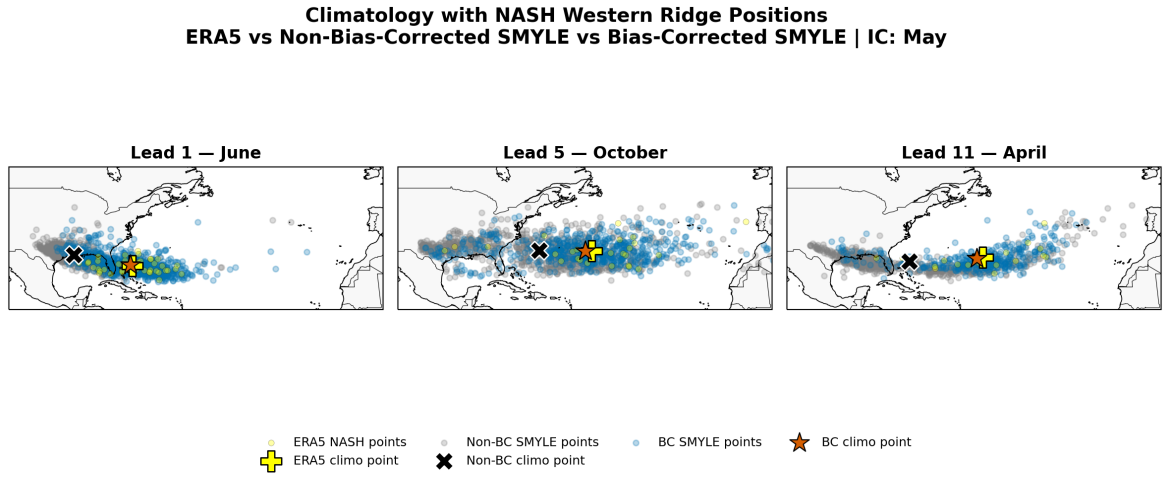
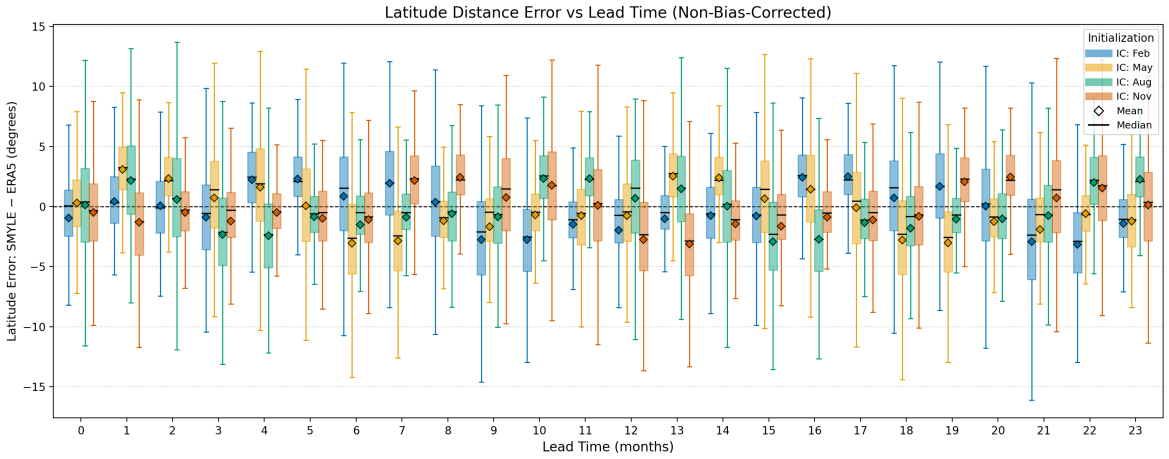


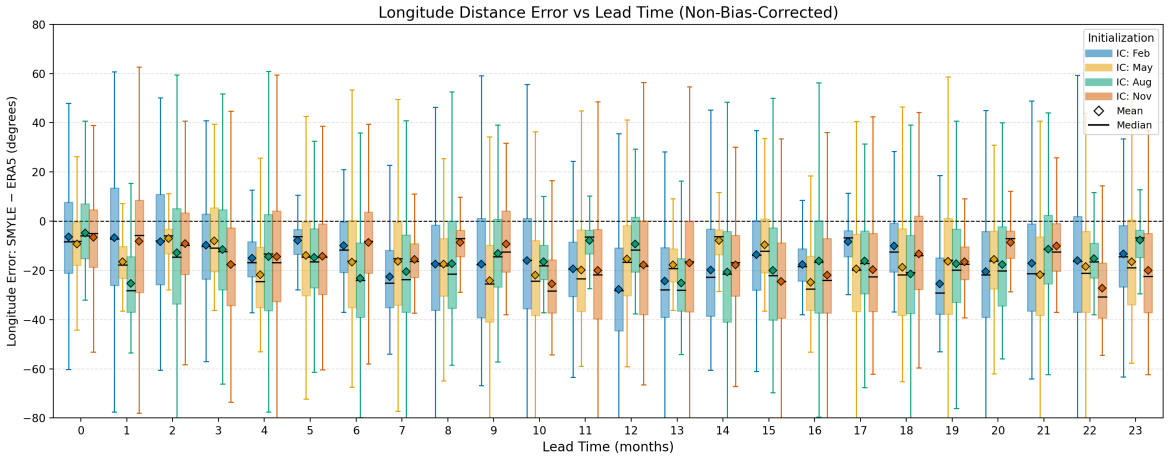
Figure 3.1: Comparison of the NASH western ridge positions and the climatological NASH western ridge position in raw SMYLE (black X), ERA5 (yellow cross), and bias-corrected SMYLE (orange star). Three leads are shown for the initialization of May over a map of the North Atlantic Ocean.

3.1.2 How Accurately Does SMYLE Predict the NASH Western Ridge Position?

After removing systematic model bias, prediction accuracy is evaluated using the displacement of the SMYLE NASH western ridge relative to ERA5 and the frequency with which SMYLE predicts the correct NASH quadrant. Continuous position errors are evaluated separately in the longitude and latitude directions, followed by quadrant-



(a)

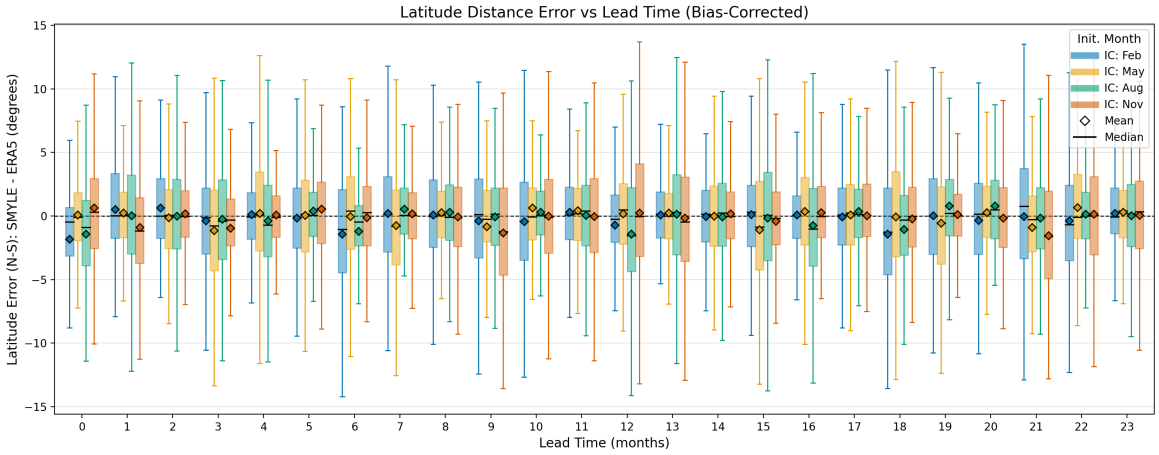


(b)

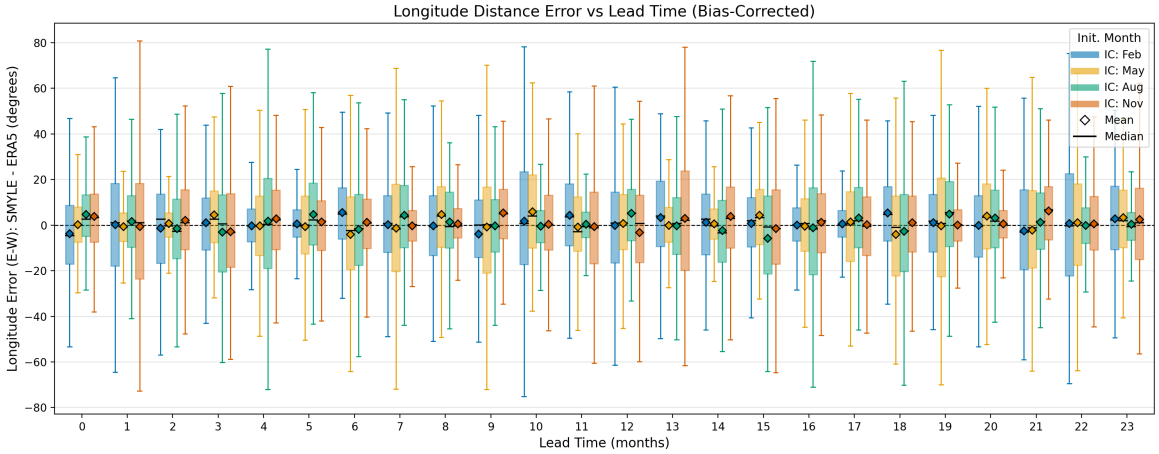
Figure 3.2: Not bias-corrected latitude (N-S)(a) and longitude (E-W)(b) distance errors for 4 initialization times (February, May, August, and November). Lead time is on the x-axis in months, and the difference (SMYLE - ERA5) in degrees is on the y-axis. The mean position error for each lead time is shown with a colored diamond, the median with a black line, and the range of ensemble difference errors (box plots). This is calculated across the years 1970-2019 and for all 20 ensembles.

based verification of the ridge configuration.

Longitude position errors are substantially larger than latitude position errors across initialization times and forecast leads (Figure 3.16). This difference is particularly evident in the ensemble spread, with a much wider distribution of east-west errors than north-south errors. Thus, although the systematic mean displacement is reduced



(a)



(b)

Figure 3.3: Bias-corrected latitude (N-S)(a) and longitude (E-W)(b) distance errors for 4 initialization times (February, May, August, and November). Lead time is on the x-axis in months, and the difference (SMYLE - ERA5) in degrees is on the y-axis. The mean position error for each lead time is shown with a colored diamond, the median with a black line, and the range of ensemble difference errors (box plots). This is calculated across the years 1970-2019 and for all 20 ensembles.

through bias correction, variability remains in the longitude of the western ridge. The longitude errors also exhibit some seasonal dependence, with larger westward errors occurring during portions of fall. In comparison, latitude position errors remain more tightly distributed around 0°, although small seasonal differences are present. These results indicate that uncertainty in the predicted NASH western ridge position is pri-

marily associated with its east-west location rather than its north-south location.

Prediction accuracy is further evaluated using the percentage of forecasts in which SMYLE predicts the same NASH quadrant as ERA5 relative to their respective climatological western ridge positions (Figure 3.4). Lead 0 consistently exhibits among the highest percentages of correct predictions across the four initializations. Although the percentage of correct predictions generally decreases with longer lead times, this decrease is not monotonic, with periods of increased quadrant agreement recurring at later lead times. The November initialization contains several leads with more than 40% correct predictions, whereas the February initialization less frequently exceeds 40%. Periods of increased quadrant agreement occur during both summer and winter, although the magnitude of these increases varies among initialization times. These results suggest that NASH quadrant prediction depends on both forecast lead and season rather than decreasing uniformly with increasing lead time.

Due to the theory that NASH has an influence on SEUS precipitation during boreal summer, quadrant prediction is examined in greater detail for the first June-August period following each initialization (Figure 3.5). Prediction accuracy differs substantially among the four western ridge quadrants. The northwest (NW) and southeast (SE) quadrants are predicted correctly more frequently than the northeast (NE) and southwest (SW) quadrants across the four initialization times. Correct prediction of the NE and SW quadrants generally remains near or below the random level, although the May initialization exhibits greater agreement for the SW quadrant than the other initialization times. These differences indicate that SMYLE prediction skill is dependent not only on season and forecast lead, but also on the particular quadrant of the NASH western ridge.

Overall, following bias correction, north-south ridge-position errors remain comparatively small, whereas east-west displacement is the dominant source of NASH western

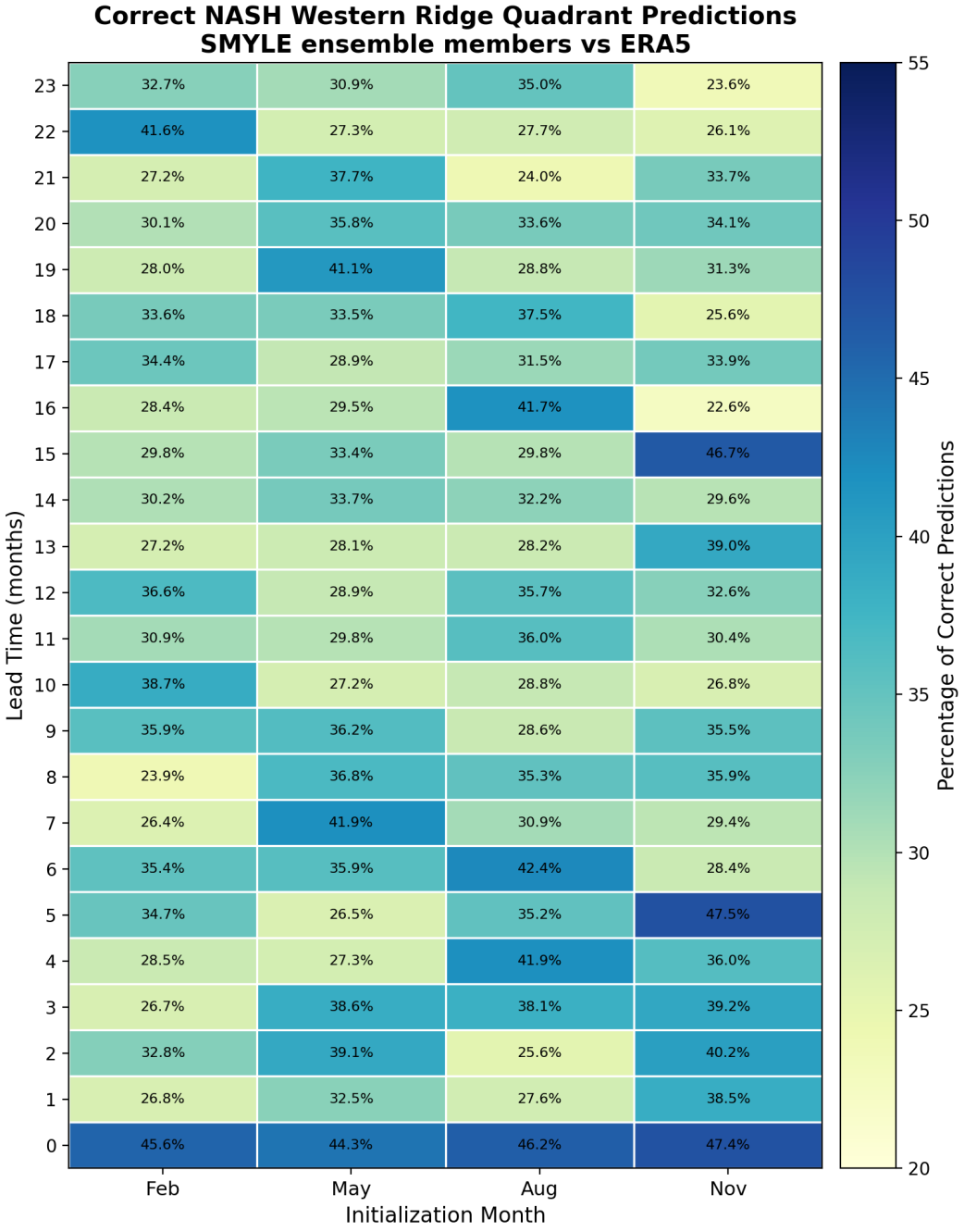


Figure 3.4: Percentage of correctly predicted NASH western ridge quadrants as a function of forecast initialization and lead time. A prediction is classified as correct when the SMYLE western ridge occurs in the same climatologically defined quadrant as the corresponding ERA5 western ridge. Shading indicates the percentage of forecasts with matching SMYLE and ERA5 quadrant classifications.

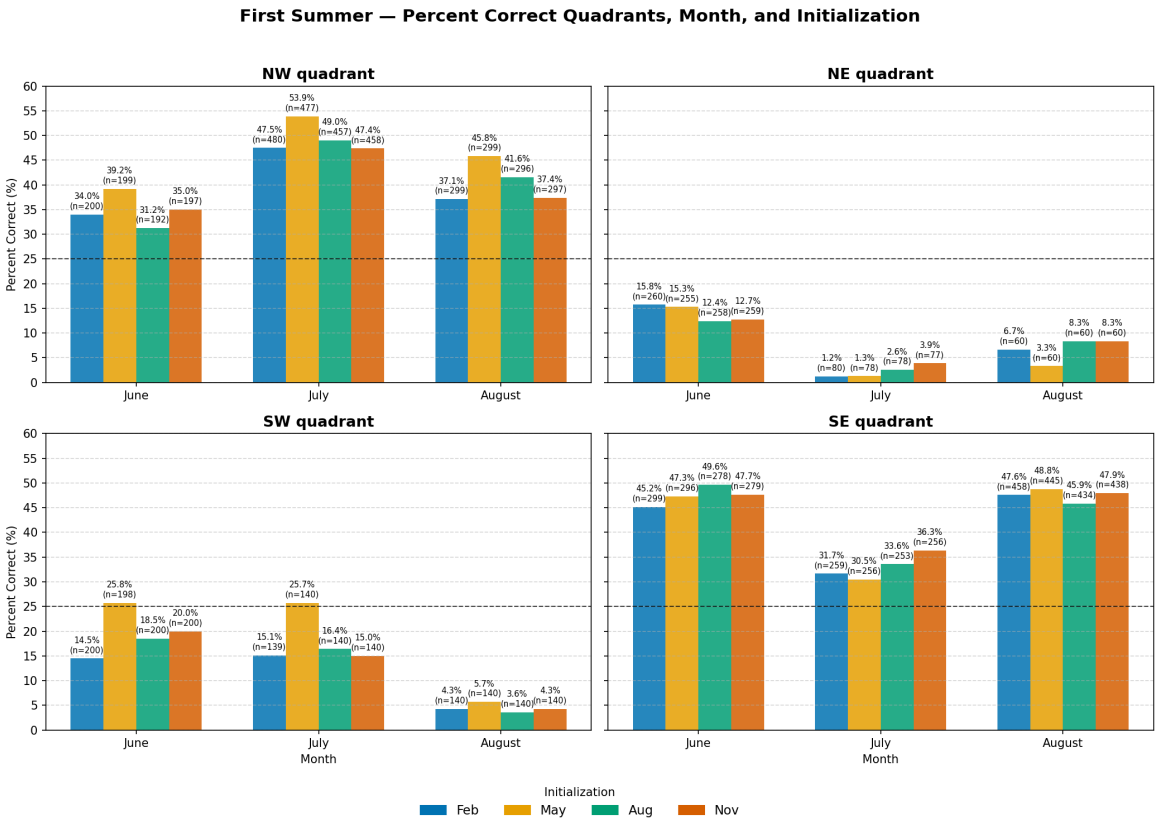


Figure 3.5: Percentage of correctly predicted NASH western ridge quadrants during the first June-August period following each SMYLE initialization. Panels correspond to the northwest (NW), northeast (NE), southwest (SW), and southeast (SE) quadrants.

ridge position error. Prediction accuracy varies with both season and forecast lead, with periods of increased quadrant agreement occurring during portions of summer and winter. Prediction skill differs among NASH configurations, with the NW and SE quadrants generally exhibiting greater agreement than the NE and SW quadrants.

The presence of the western-ridge prediction skill raises the question of whether skillful prediction of the large-scale circulation is accompanied by skillful precipitation prediction over the SEUS.

3.2 How Well Does SMYLE Predict Precipitation?

This section addresses the second research question by evaluating the performance of SMYLE precipitation forecasts. The ability of the model to distinguish above-average from below-average precipitation is assessed together with the accuracy and reliability of the forecast probabilities.

3.2.1 Deterministic and Probabilistic Precipitation Performance

The Brier Score (BS) measures the accuracy of probabilistic precipitation forecasts, with lower values indicating smaller forecast errors and zero representing a perfect forecast. SMYLE BS is compared with the CHIRPS climatological reference BS in Figure 3.6.

Across the four initialization times, SMYLE BS generally remains close to the CHIRPS climatology, with values ranging approximately from 0.22 to 0.27 (Figure 3.6). There is no consistent pattern of improvement over climatology across forecast leads. The August and February initializations contain occasional leads for which the SMYLE BS is lower than the climatological BS, while the May and November initializations begin with lower BS values than their respective climatological references before exhibiting substantial variation across subsequent leads. The February initialization generally exhibits higher BS values relative to climatology and rarely outperforms the reference forecast. Overall, the proximity of the SMYLE and climatological BS indicates that SMYLE precipitation probabilities generally provide limited improvement over the climatological probability forecast.

The Brier Skill Score (BSS) directly quantifies this performance relative to the CHIRPS climatological reference, with positive values indicating improvement over climatology and negative values indicating poorer performance (Figure 3.7). Positive

BSS values occur infrequently across the four initialization times, while many forecast leads exhibit negative BSS values below -0.10. Thus, although the magnitude of the BS varies among initialization times and leads, SMYLE generally does not improve upon the climatological probability forecast for above-average precipitation.

Forecast reliability is evaluated by comparing the predicted probability of above-average precipitation with its observed frequency in CHIRPS (Figure 3.8). Across the four initialization times, lead 0 generally lies closest to the one-to-one line representing perfect reliability. At lower forecast probabilities, SMYLE generally lies above the one-to-one line, indicating that the observed frequency of above-average precipitation is greater than the forecast probability and that SMYLE under-forecasts the event probability. At higher forecast probabilities, portions of the reliability curves fall below the one-to-one line, indicating over-forecasting of the probability of above-average precipitation. The May initialization generally remains closer to the perfect-reliability line across the selected leads, whereas the February initialization exhibits greater departures from perfect reliability. These results indicate that the correspondence between forecast probability and observed frequency varies with both initialization and forecast lead.

Despite limited reliability and Brier skill, the forecasts can still contain information about whether above-average precipitation is more likely to occur. This discrimination is evaluated using the area under the receiver operating characteristic curve (ROC AUC; Figure 3.9). ROC AUC values of 0.5 indicate no discrimination, whereas values greater than 0.5 indicate an ability to distinguish between above-average and below-average precipitation events. Although some leads have AUC values at or below 0.5, the majority remain between approximately 0.5 and 0.7. Leads falling below 0.5 generally remain above approximately 0.45. SMYLE therefore contains some discriminatory information for above-average precipitation at many forecast leads, but the magnitude

of this discrimination is generally weak to moderate.

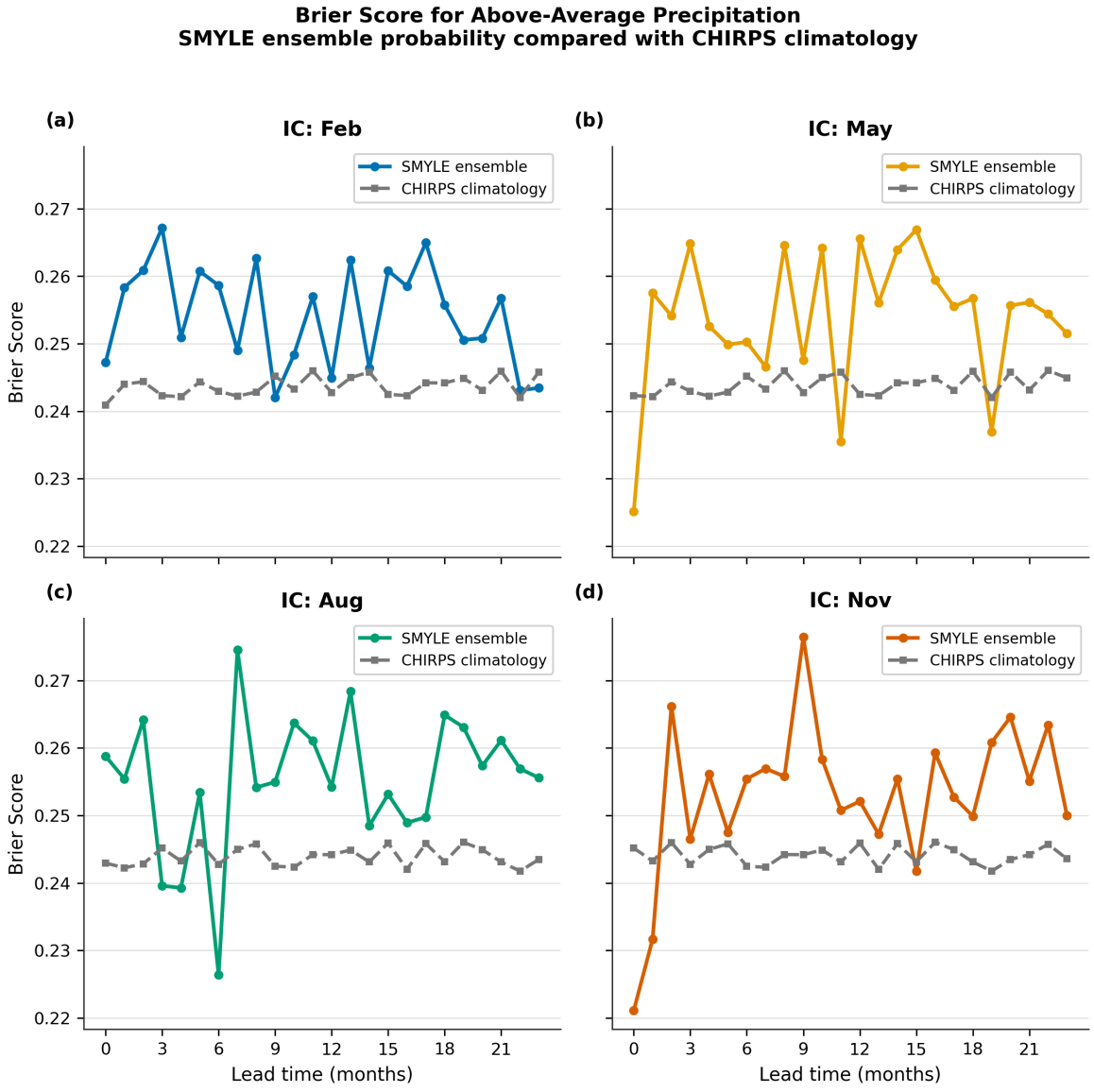


Figure 3.6: Brier Score (BS) for probabilistic SMYLE forecasts of above-average precipitation as a function of lead time for each initialization. The respective solid color line represents the SMYLE ensemble Brier score and the gray dashed line represents the CHIRPS climatology Brier score.

Overall, SMYLE exhibits limited probabilistic skill for SEUS precipitation. Although the forecast contains information that can distinguish between above- and below-average events, its probabilities are not sufficiently reliable to consistently out-

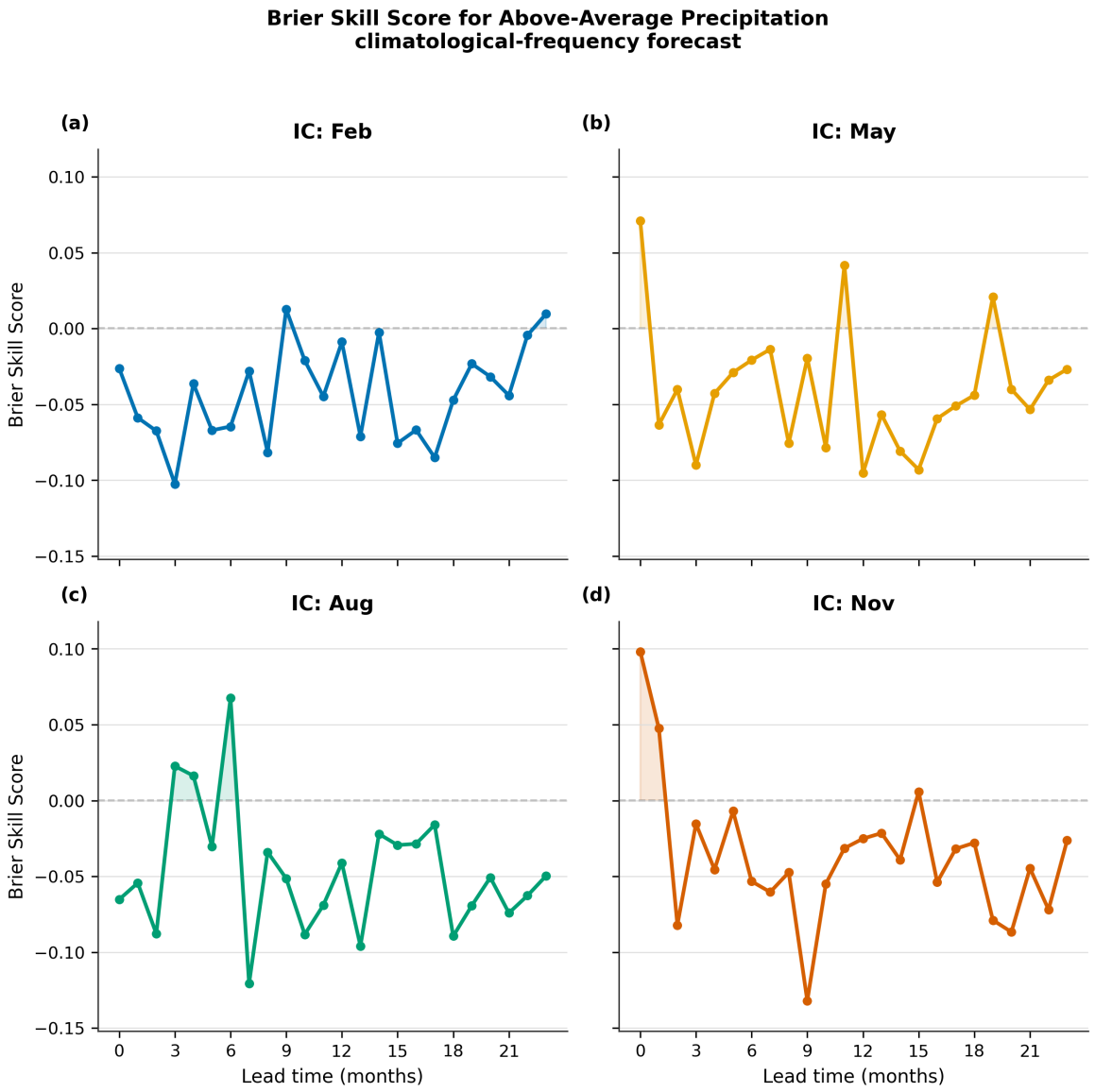


Figure 3.7: Brier Skill Score (BSS) for probabilistic SMYLE forecasts of above-average precipitation as a function of lead time for each initialization. The BSS reference forecast is the observed CHIRPS climatological probability of above-average precipitation for each calendar month and grid point. Positive BSS values indicate skill relative to climatology, whereas negative values indicate lower skill than climatology.

perform the CHIRPS climatological reference. The limited precipitation skill motivates testing whether forecast performance depends on the accuracy of the predicted large-scale circulation. In particular, precipitation prediction may improve when SMYLE

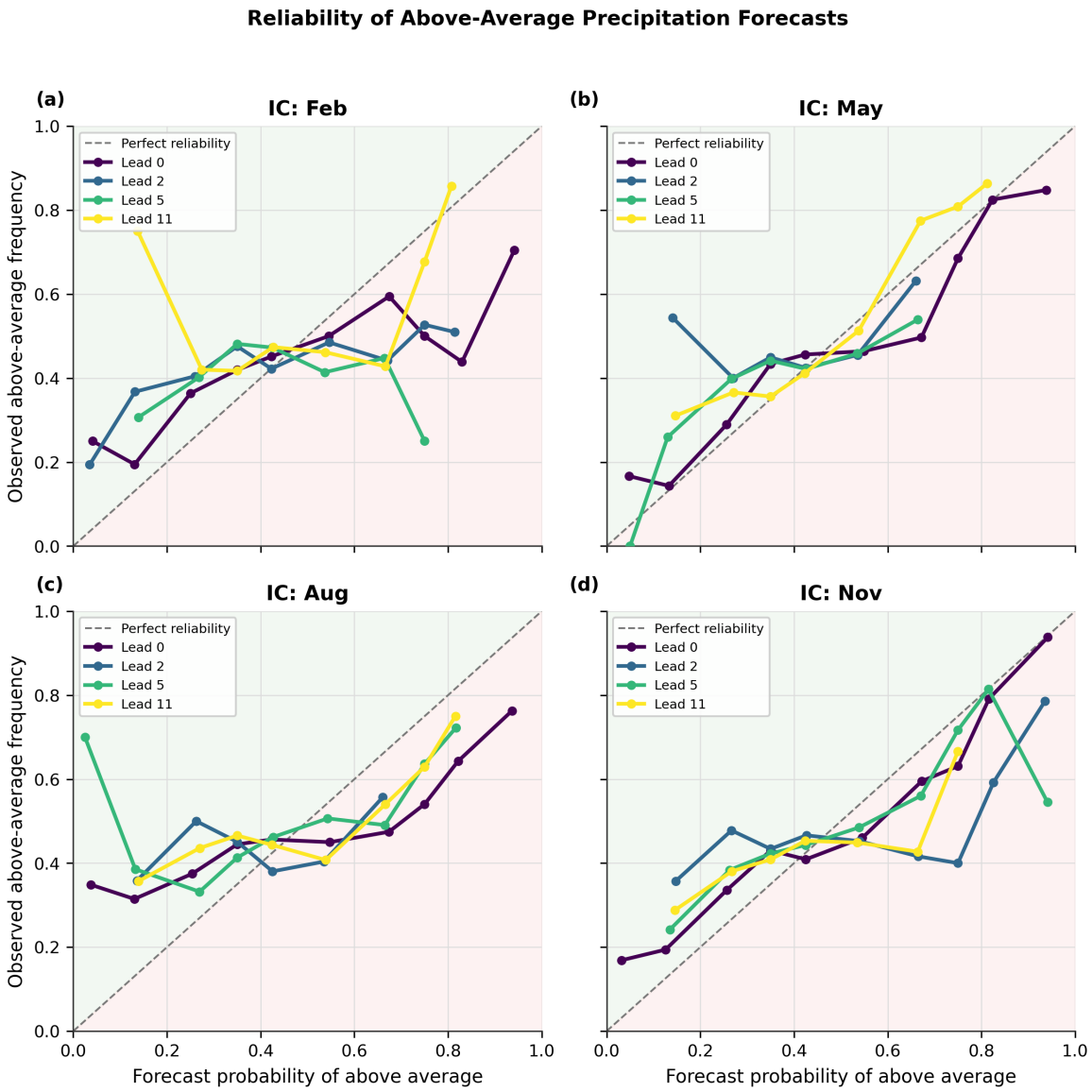


Figure 3.8: Reliability diagram for selected lead times of SMYLE probabilistic forecasts of above-average precipitation. Forecast probabilities are compared with the observed frequency of above-average precipitation from CHIRPS. Green shading represents underforecasting the probability, and red represents overcasting the probability. The one-to-one line represents perfect reliability.

correctly predicts the NASH western ridge quadrant.

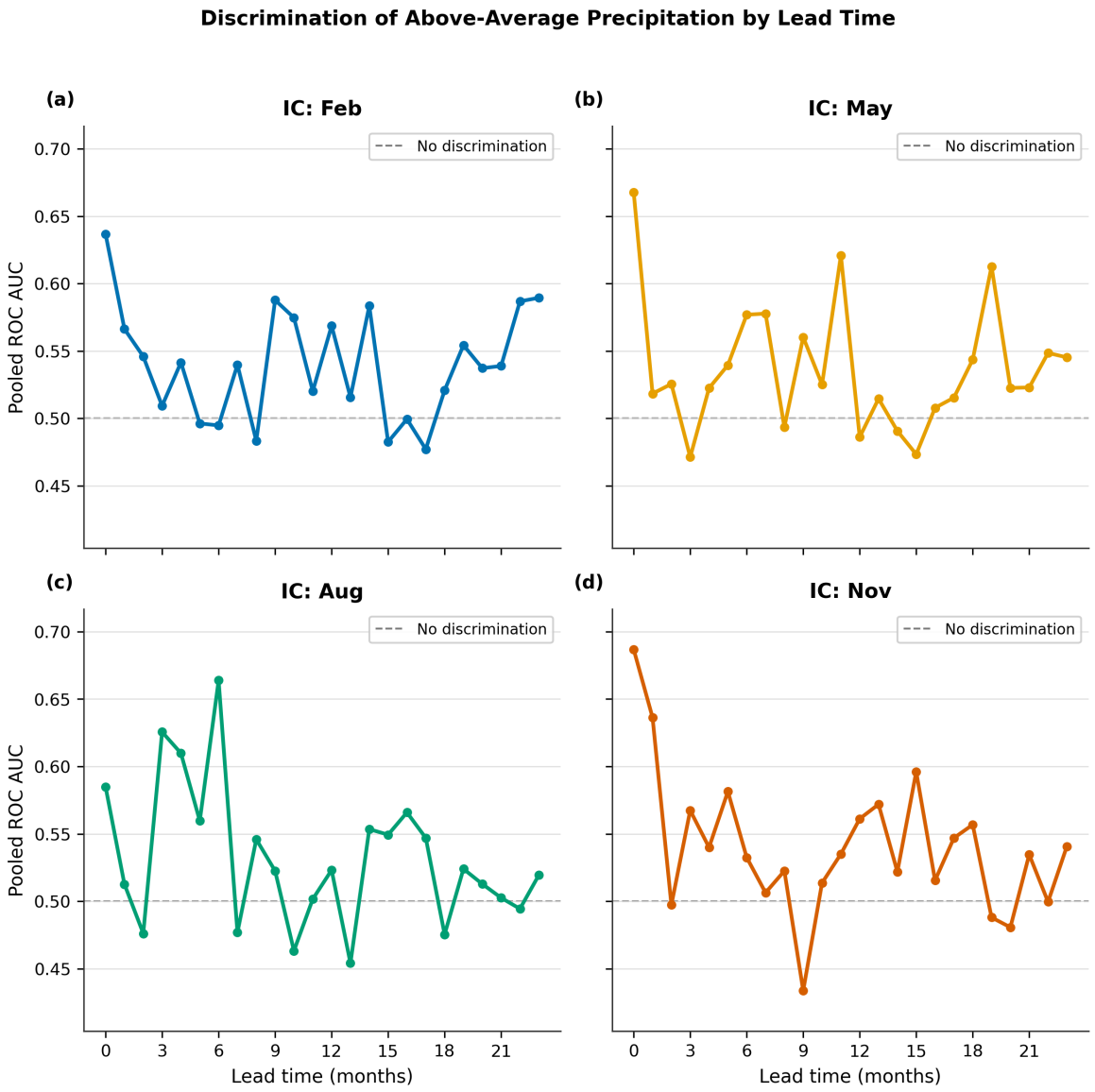


Figure 3.9: Area under the receiver operating characteristic curve (ROC AUC) for pooled SMYLE forecasts of above-average precipitation as a function of forecast lead for each initialization. An AUC of 0.5 indicates no discrimination between above-average and below-average precipitation events, while values greater than 0.5 indicate increasing discriminatory ability.

3.3 Does Correct NASH Western Ridge Prediction Improve SEUS Precipitation Prediction?

This section addresses the third research question by comparing precipitation forecast performance between cases in which the NASH western ridge quadrant is correctly and incorrectly predicted. Ensemble-size matching is applied to ensure that differences between the two groups do not arise solely from differences in sample size.

3.3.1 Does Correct NASH Prediction Improve Probabilistic Skill?

When evaluated using equal ensemble sizes and common verification years, ensemble members that correctly predict the NASH generally produce more accurate precipitation probabilities than members that incorrectly predict the NASH (Figure 3.10). For most lead times across initializations, NASH correct has a lower Brier score than NASH incorrect. Often, in fall and spring, NASH correct tends to have a higher score than NASH incorrect. In contrast, during some winter and summer months, NASH correct tends to be close to or lower than the all-members line and the climatology line but rarely passes those lines. Therefore, conditioning on NASH correctness does not consistently outperform the full ensemble, indicating that NASH prediction provides useful information but is not sufficient by itself to produce the most skillful precipitation forecast. However, this analysis does not consider that NASH correctness is based on ensemble matching, while the all-member line is the full 20 ensembles for paired years. Therefore, to determine whether improvements associated with correct NASH prediction exceed those expected from ensemble-size reduction alone, the Brier Score of the NASH-correct subset was compared with the expected Brier Score of an equally

sized random subset of the full ensemble in Figure 3.11. Negative differences indicate that NASH-correct member selection reduces precipitation probability error beyond that expected from arbitrary member selection, while positive differences indicate no added benefit from conditioning on NASH correctness. The majority of the leads did provide an improvement to BS when conditioned on correct NASH, and in the leads where there is a large increase in positive delta where there is no added value, the number of ensembles was small in comparison. This means those large increases could be due to the ensemble size rather than the NASH not providing value. The months of no value mostly occur during the spring and fall, corresponding in Figure 3.10 to the seasons where NASH correct is higher in Brier score than NASH incorrect.

Although NASH-correct members generally exhibited lower Brier Scores than NASH-incorrect members at several leads, conditional Brier Skill Scores remained predominantly negative, indicating that the improvement associated with correct NASH representation was generally insufficient to outperform the CHIRPS climatological reference.

Overall, correctly predicting the NASH improves precipitation forecast performance relative to incorrectly predicting the NASH, although the full ensemble remains more accurate overall. The full ensemble benefits from more members and averaging over a wider range of outcomes. The improvement associated with correct NASH prediction was more consistent across the warm and cold seasons, whereas several transitional-season leads showed reversed differences.

3.3.2 How Does Correct NASH Prediction Affect Precipitation Forecasts?

Member-level precipitation agreement conditioned on NASH prediction accuracy is shown in Figure 3.12. Across the majority of forecast leads, ensemble members that cor-

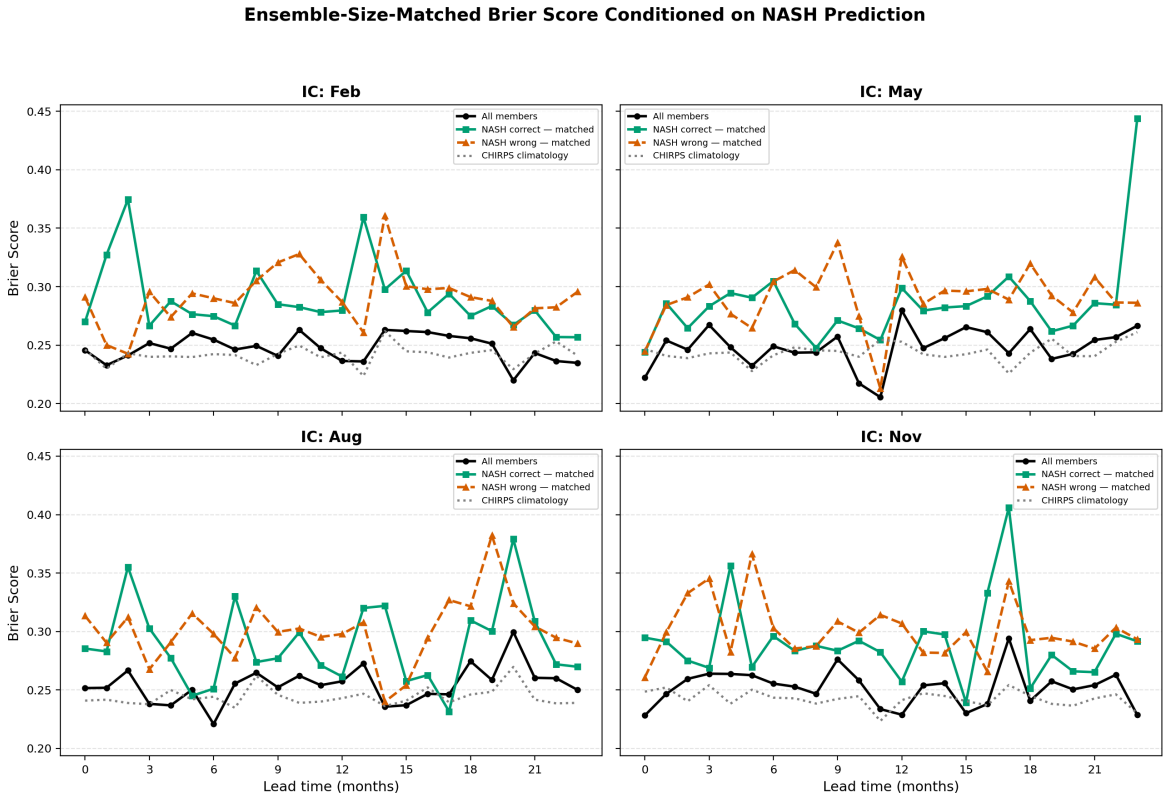


Figure 3.10: Brier Score for above-average precipitation forecasts conditioned on correct (solid green line) and incorrect prediction (dashed orange line) of the NASH western ridge quadrant for the 4 initializations by lead time (month, x-axis). Results are compared with the corresponding full-ensemble precipitation forecast. CHIRPS climatology (dotted gray line) and all members (solid black line) are present for comparison.

rectly predict the NASH western ridge quadrant have a higher percentage of precipitation-category agreement than members that incorrectly predict the NASH quadrant. This indicates that correct representation of the NASH is generally associated with improved classification of above- and below-average SEUS precipitation. Although NASH-correct members generally exhibit greater precipitation agreement, this relationship reverses at several leads, demonstrating that correct NASH quadrant prediction is not sufficient for correctly predicting precipitation. Also, precipitation agreement remains below 50 percent at several leads, demonstrating that correctly predicting the NASH quadrant does not necessarily result in a correct precipitation classification. These periods of

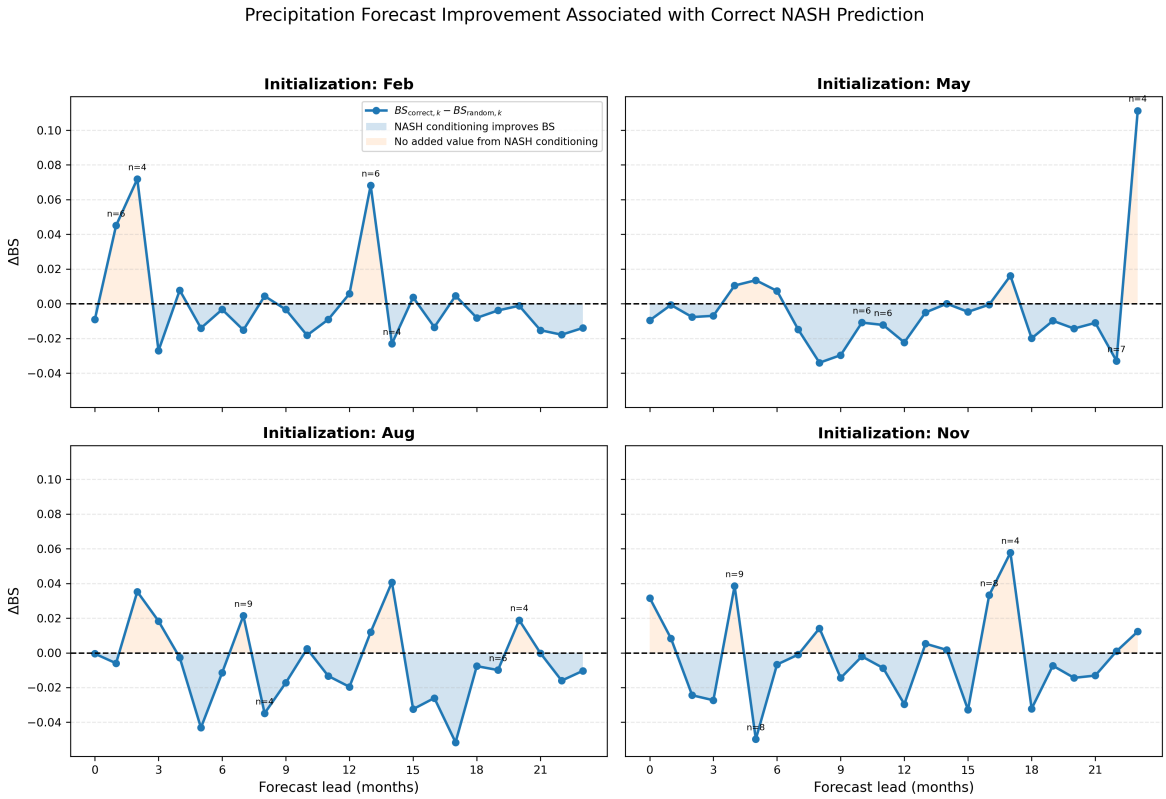


Figure 3.11: Brier Score difference for above-average precipitation forecasts conditioned on correct prediction of the NASH western ridge quadrant and an equally sized random subset of the full ensemble for the 4 initializations by lead time (month, x-axis). Negative areas are shaded blue to show NASH conditioning improves BS, and the positive difference is shaded in orange to show that no added value occurred from NASH conditioning. Leads with fewer than 10 matched years are annotated.

lower agreement occur primarily during spring and fall, although the relationship varies among initialization times and individual leads. Conversely, several transitional-season leads exhibit relatively high agreement, indicating that the relationship is not governed solely by season. Overall, the results suggest that the correct prediction of NASH is associated with improved agreement between precipitation categories, but the strength and consistency of this relationship depend on the lead and initialization of the forecast.

Examining reliability conditioned on NASH quadrant prediction for lead 0 (Figure 3.14), the NASH-correct and NASH-incorrect forecasts exhibit variability across

the four initializations. The May initialization and the NASH-correct forecasts for the August initialization generally follow the 1:1 line, indicating relatively good reliability. All four initializations show a mixture of under- and over-prediction, with forecast probabilities falling on both sides of the 1:1 line. Overall, the reliability of precipitation forecasts conditioned on NASH correctness varies by initialization, suggesting that correctly predicting the NASH does not consistently produce well-calibrated precipitation probabilities.

Generally, precipitation discrimination is improved when the NASH is correctly predicted (Figure 3.15), with NASH-correct members exhibiting a higher pooled ROC AUC across the four initializations. However, this improvement is seasonally dependent. NASH-correct members most consistently outperform the all-member and NASH-incorrect members during summer and winter, whereas NASH-correct ROC AUC occasionally falls below both groups during spring and fall. In contrast, NASH-incorrect members generally track or fall below the all-member ROC AUC, indicating reduced ability to discriminate between above-average and non-above-average precipitation when the NASH is incorrectly predicted. These results suggest that accurate representation of the NASH contributes to precipitation discrimination, particularly during the seasons when the NASH has the most influence over southeast circulation and precipitation. The seasonal dependence of this relationship indicates that correct NASH quadrant prediction alone does not guarantee improved precipitation discrimination. This motivates further exploration of the magnitude and direction of western-ridge position errors and their associated circulation and precipitation patterns.

The spatial distribution of the difference in member-level precipitation agreement between NASH-correct and NASH-incorrect members for lead 0 is shown in Figure 3.13. Values greater than zero indicate grid points where precipitation-category agreement

is greater among members that correctly predict the NASH quadrant, while values less than zero indicate greater agreement among members that incorrectly predict the NASH quadrant. February initiation shows a predominance of negative differences in the western portion of the domain, indicating greater precipitation agreement among NASH-incorrect members in this region. In contrast, August initiation exhibits more widespread positive differences, with precipitation agreement generally greater among NASH-correct members. The May and November initiations show a more spatially mixed pattern, with positive and negative differences occurring throughout the domain. These results indicate that the association between correct NASH prediction and precipitation agreement is not spatially uniform. Thus, although correct NASH prediction is generally associated with improved precipitation agreement, the NASH western ridge placement alone does not consistently explain the spatial distribution of precipitation prediction accuracy.

Correct prediction of the NASH is associated with improved precipitation-category agreement, discrimination, and probabilistic accuracy relative to cases in which the NASH is incorrectly predicted. However, conditioning on NASH correctness does not consistently outperform either the full ensemble or the climatological forecast. Accurate prediction of the NASH western ridge therefore provides useful information for SEUS precipitation prediction but is not sufficient by itself to produce a skillful precipitation forecast. The persistence of precipitation errors even when the NASH western ridge is correctly predicted indicates that additional sources of forecast error remain. This raises a second question: when the precipitation forecast remains incorrect, which aspects of the predicted NASH circulation differ from observations? The following composites therefore move beyond binary quadrant correctness and examine the magnitude and direction of western-ridge position errors and their associated circulation and precipitation patterns.

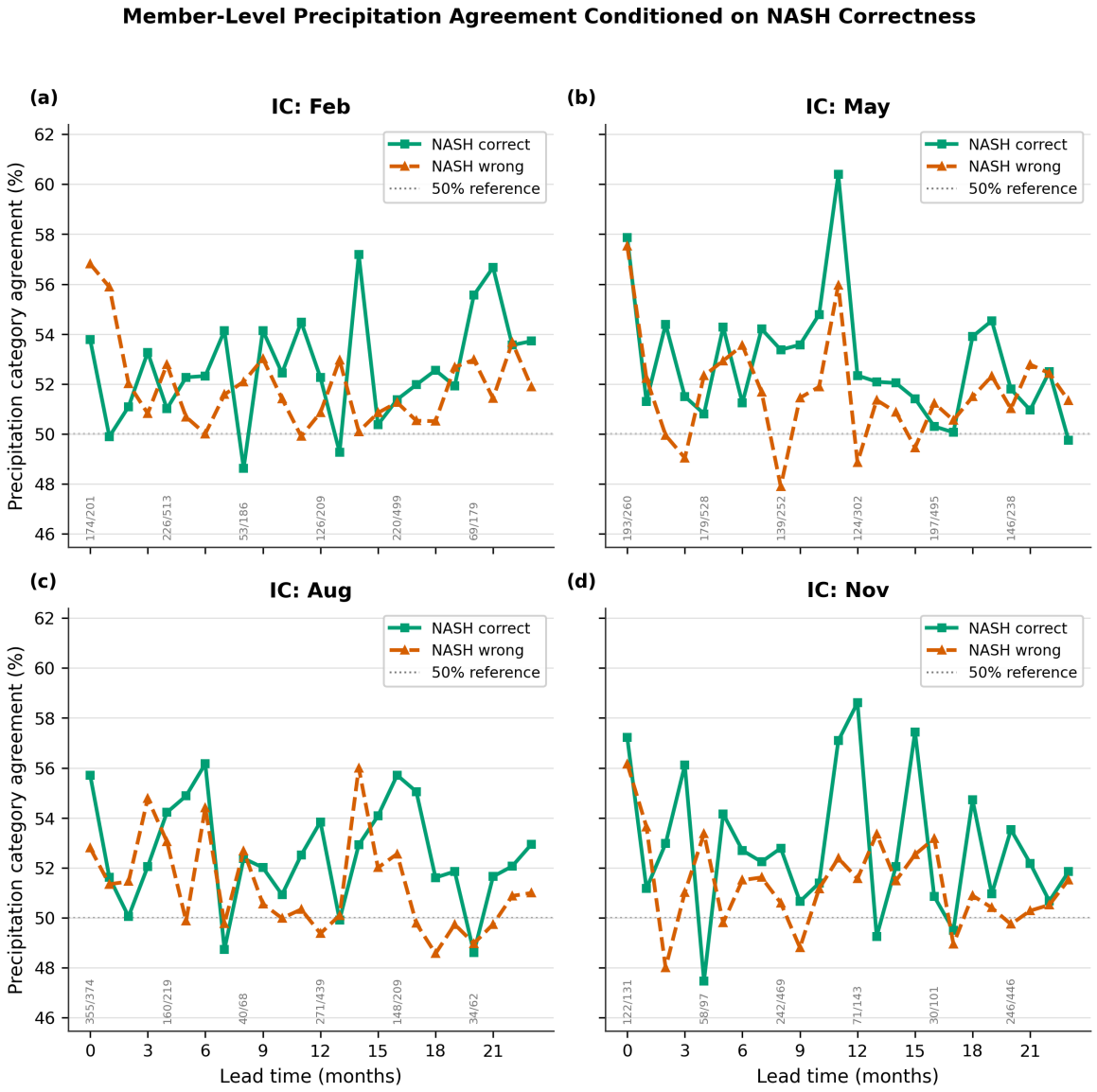


Figure 3.12: Agreement between SMYLE and CHIRPS precipitation categories when the NASH western ridge quadrant is correctly (solid green line) and incorrectly (dashed orange line) predicted in percentages per lead time(months). The 4 initializations are represented in the panels. Gray annotations indicate the number of member-level samples used for the NASH-correct and NASH-incorrect groups, respectively (correct/incorrect).

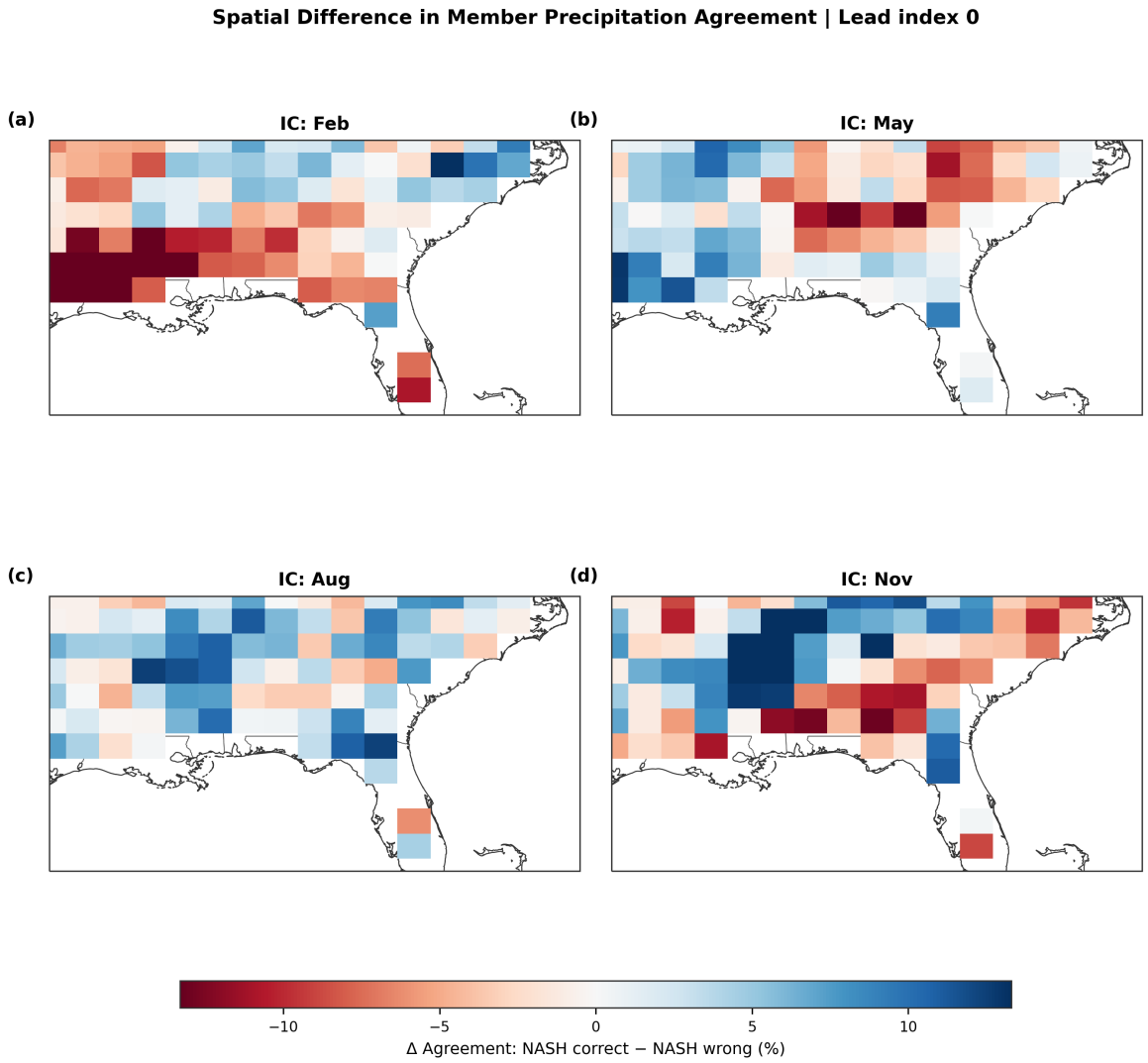


Figure 3.13: Spatial distribution of precipitation forecast performance conditioned on the accuracy of the predicted NASH western ridge quadrant. The 4 initializations are represented in the panels, and positive values (blue) indicate greater precipitation accuracy among NASH-correct members.

3.4 What Limits Prediction Skill?

This section examines why SEUS precipitation remains difficult to predict even when the large-scale NASH circulation is represented correctly. Differences in the circulation, western ridge position, moisture transport, and regional precipitation fields are evalu-

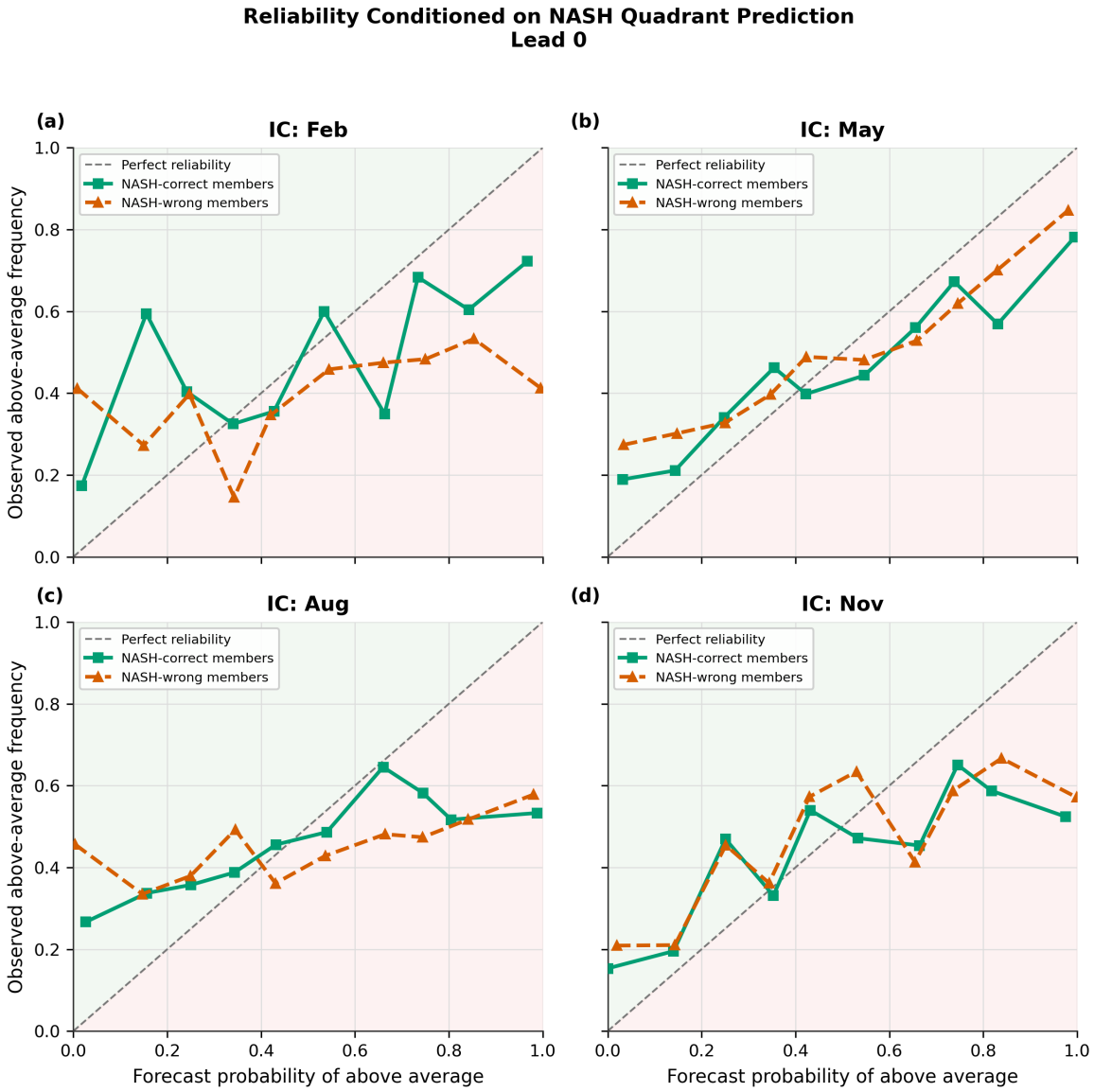


Figure 3.14: Reliability of probabilistic above-average precipitation forecasts conditioned on correct (solid green line) and incorrect (dashed orange line) NASH western ridge prediction. Forecast probabilities are compared with the observed frequency of above-average precipitation from CHIRPS.

ated to determine which errors persist after conditioning on correct NASH prediction.

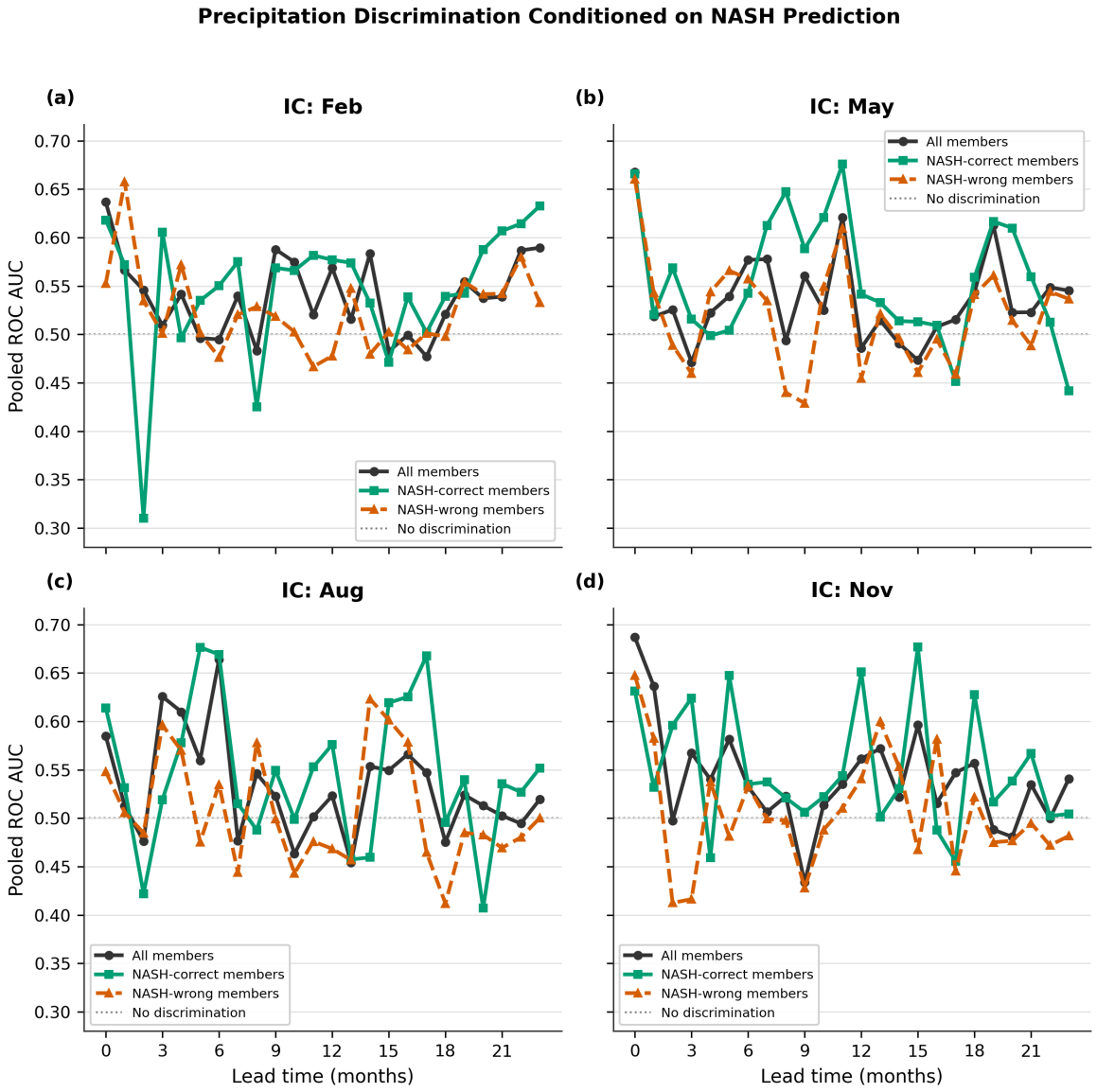


Figure 3.15: Receiver operating characteristic (ROC) curves for precipitation forecasts conditioned on correct (solid green line) and incorrect (dashed orange line) prediction of the NASH western ridge quadrant per lead time (months). The area under each curve summarizes the ability of each forecast subset to discriminate between above-average and below-average precipitation events.

3.4.1 Errors Despite Correct Circulation

Figure 3.16 further demonstrates how errors in the predicted NASH western ridge position are related to circulation and precipitation errors over the southeastern United

States. The excellent western-ridge error category ($< 1°$) contains substantially fewer cases than the other distance-error categories. Despite the close agreement between the SMYLE and ERA5 western ridge locations in these cases, SMYLE exhibits a positive precipitation anomaly difference over portions of the region, indicating that accurately predicting the western ridge location alone does not guarantee an accurate precipitation response. In comparison, the good and moderate distance-error categories exhibit precipitation anomaly differences that are generally closer to zero. The larger apparent precipitation bias in the excellent category should be interpreted cautiously because of its considerably smaller sample size ($n = 58$), which makes its composite more sensitive to individual cases.

The poor category ($> 10°$) contains the largest number of cases and is characterized by a substantial separation between the mean SMYLE and ERA5 western ridge locations. The mean western ridge markers do not necessarily fall directly on the 1560-m contour of the composite height field, even though each western ridge position was diagnosed from the intersection of the 1560-m geopotential-height contour and the zero-zonal-wind contour. This occurs because the plotted markers represent the mean of western ridge positions diagnosed independently for each forecast case, whereas the contours represent the mean of the corresponding geopotential-height fields. The greater displacement of the mean ridge marker from the composite 1560-m contour in the poor category is consistent with the larger spatial variability expected among these cases.

Interestingly, the poor western ridge category does not exhibit the largest precipitation anomaly differences, despite containing cases with western ridge position errors greater than 10°. Instead, the composite precipitation difference remains relatively small across much of the domain. Therefore, there is not a simple monotonic relationship between total western ridge position error and the magnitude of the composite

precipitation error. One possible explanation is that the total-distance metric combines western ridge errors occurring in different directions, which may be associated with different precipitation responses. This becomes clearer when the longitudinal component in Figure 3.18 of the western ridge error is considered separately. When SMYLE predicts the western ridge too far east, precipitation is generally wetter relative to CHIRPS, whereas a westward displacement is associated with generally drier conditions. Thus, the direction of the western ridge displacement, particularly in longitude, appears to provide more information about the associated precipitation-error pattern than the magnitude of the total position error alone.

The longitude-error composites provide a clearer physical relationship between NASH displacement and precipitation errors. When the SMYLE western ridge is displaced eastward relative to ERA5, SMYLE generally produces wetter precipitation anomalies, whereas a westward displacement is associated with predominantly drier precipitation anomalies across much of the region. When the western ridge longitude is close to ERA5, the composite precipitation anomaly difference is generally near zero. This systematic change in the sign of the precipitation error with longitudinal ridge displacement suggests that the east–west placement of the western ridge may be particularly important for the circulation and moisture-transport patterns affecting southeastern U.S. precipitation. Although bias correction improves the mean geopotential-height field and diagnosed western ridge position, it does not alter the underlying model dynamics or physical parameterizations. Consequently, residual errors in ridge amplitude, geopotential-height gradients, low-level circulation, moisture transport, and regional precipitation processes can remain even after the mean-state bias is removed.

The correct-versus-incorrect quadrant composites further illustrate that correctly classifying the NASH western ridge into a quadrant does not imply an exact repre-

sentation of the associated circulation. When the quadrant classification is correct, precipitation anomaly error over the domain is generally more negative, while the quadrant incorrect has positive shading. The SMYLE and ERA5 geopotential-height fields may remain broadly similar even when the quadrant classification is incorrect because quadrant correctness depends on the western ridge position relative to the climatological latitude and longitude boundaries. Thus, relatively small or spatially localized differences near the western ridge can change the quadrant classification while the large-scale Z850 patterns remain similar. Conversely, a correctly predicted quadrant can still contain errors in the precise western ridge position, ridge amplitude, height gradients, and low-level circulation. These residual circulation errors provide a physical explanation for why precipitation skill can remain imperfect even when the NASH quadrant is correctly predicted.

These results demonstrate that classification of the NASH western ridge into the correct quadrant does not imply that the complete circulation is accurately represented. Residual differences in ridge position, circulation strength, and moisture transport can remain even when the NASH western ridge quadrant is correct. Consequently, accurate NASH prediction can increase the likelihood of improved SEUS precipitation forecasts but does not uniquely determine regional precipitation.

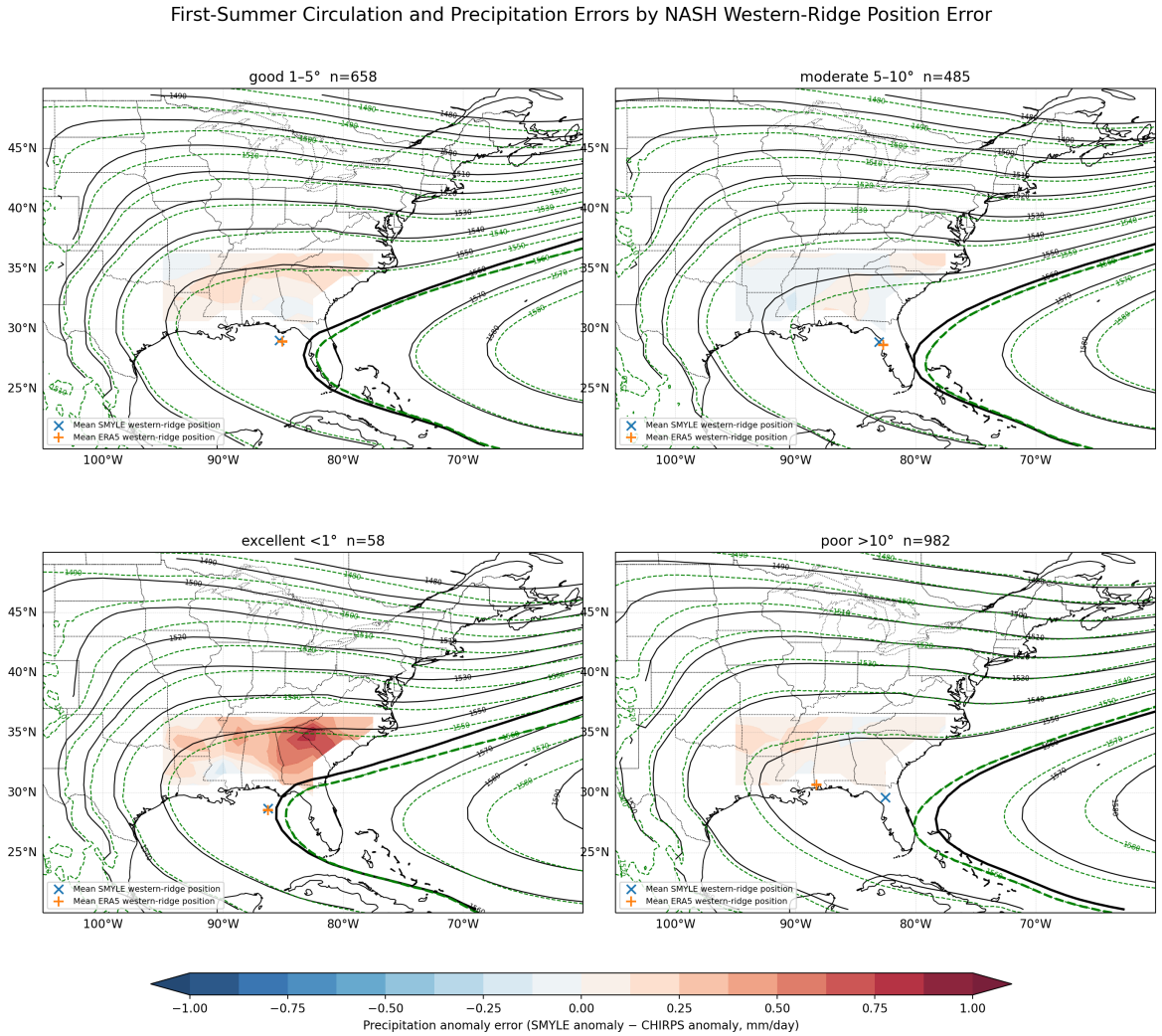


Figure 3.16: May initialization first-summer circulation and precipitation errors by NASH western-ridge position error. SMYLE 850 hPa bias-corrected (black line) and ERA5 850 hPa (dashed green line), precipitation anomaly differences (colorbar, mm/-day), mean SMYLE western ridge position (blue X), and mean ERA5 western ridge location (orange cross) for forecasts separated by NASH western ridge point distance error bin (poor, moderate, good, and excellent).

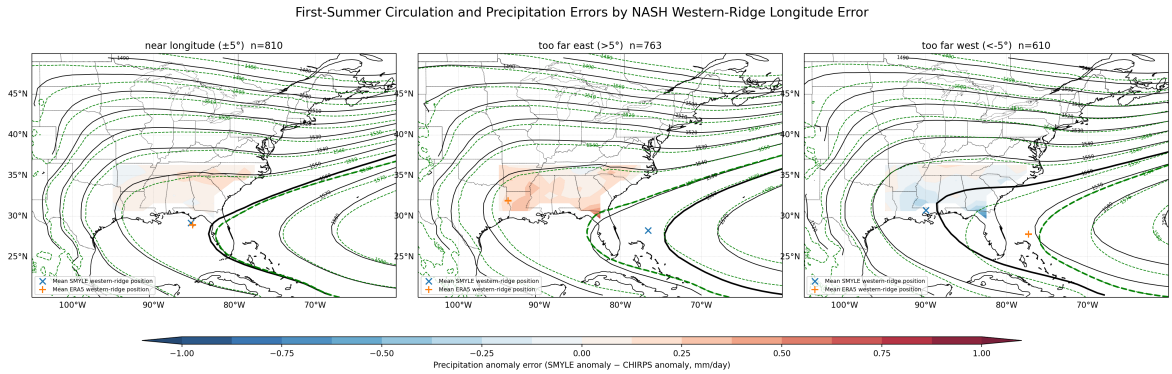


Figure 3.17: May initialization first summer circulation and precipitation error by NASH western-ridge longitude error. SMYLE 850 hPa bias-corrected (black line) and ERA5 850 hPa (dashed green line), precipitation anomaly differences (colorbar, mm/-day), mean SMYLE western ridge position (blue X), and mean ERA5 western ridge location (orange cross) for forecasts separated by NASH western ridge point longitude-error bin (too far west, near longitude, too far east)

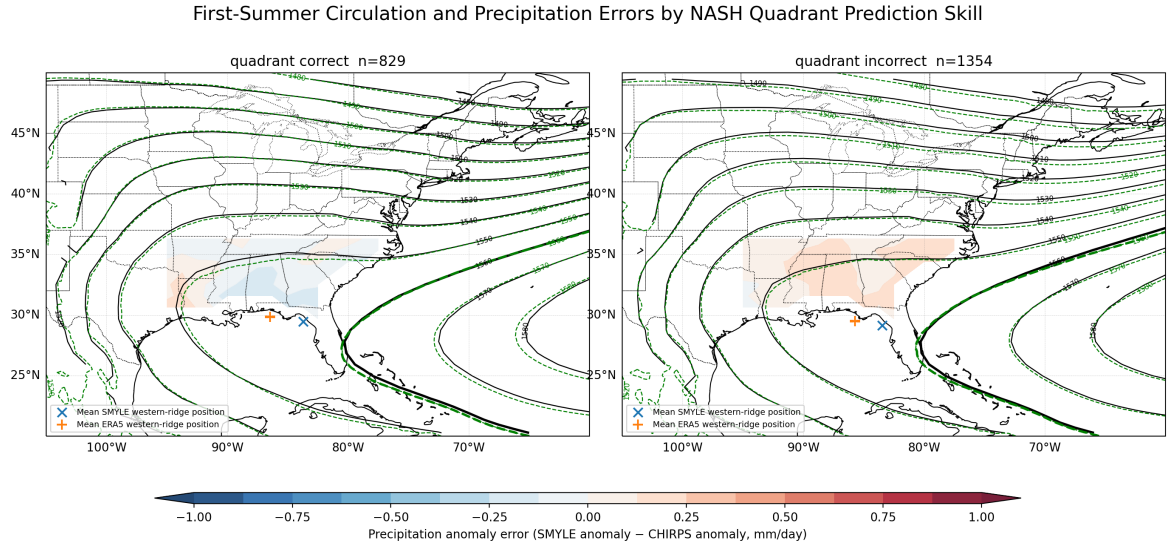


Figure 3.18: May initialization first-summer circulation and precipitation errors by NASH quadrant prediction skill. SMYLE 850 hPa bias-corrected (black line) and ERA5 850 hPa (dashed green line), precipitation anomaly differences (colorbar, mm/day), mean SMYLE western ridge position (blue X), and mean ERA5 western ridge location (orange cross) for forecasts separated by NASH western ridge quadrant prediction.

Chapter 4

Discussion and Conclusions

4.0.1 Discussion

The results of this study demonstrate that seasonal-to-multi-year variability of the North Atlantic Subtropical High (NASH) western ridge can be predicted to some extent in an initialized climate model, particularly during boreal summer. However, this circulation predictability does not translate directly into comparable skill in Southeast United States (SEUS) precipitation. Together, these results highlight an important distinction between the predictability of a large-scale circulation feature and the predictability of its regional hydroclimatic impacts. While SMYLE captures meaningful variability in NASH western ridge position, precipitation remains influenced by additional circulation, moisture, land- atmosphere, and mesoscale processes that are not fully represented by western ridge position alone.

4.1 What Have We Learned About NASH Western Ridge Prediction Skill?

Previous studies have shown that variability in the NASH western ridge is characterized by substantial zonal displacement, with comparatively smaller meridional shifts (Li et al., 2011). The results of this study are consistent with this behavior. Across

the SMYLE hindcasts, errors in western ridge longitude were substantially larger than errors in latitude, indicating that uncertainty in the predicted NASH position is dominated by east-west displacement. Even after correcting the systematic mean-state bias in the SMYLE circulation fields, errors in western ridge position remained. Therefore, the primary uncertainty in predicting the NASH western ridge is not simply whether the model can reproduce its latitude, but how far east or west the ridge extends.

NASH prediction skill also exhibits a strong seasonal dependence rather than a simple monotonic degradation with increasing forecast lead time. Western ridge position is generally better represented during summer, when positional errors are reduced and quadrant prediction skill increases. In contrast, spring forecasts exhibit substantial zonal displacement even when quadrant classification remains above the random-chance expectation, while fall generally contains some of the largest longitudinal errors across initializations. Winter exhibits comparatively smaller positional errors and elevated quadrant prediction percentages. The recurrence of these patterns across initialization months suggests that NASH forecast performance depends on the season being predicted in addition to forecast lead time.

This seasonal behavior is physically relevant because the NASH intensifies during boreal summer and its western ridge becomes particularly important for SEUS hydroclimate (Li et al., 2019). Previous work has also suggested that changes in the seasonal evolution of the NASH may cause westward extension to occur earlier in the year under a warming climate (Song et al., 2018). The pronounced seasonal differences identified here therefore emphasize the importance of evaluating NASH prediction by target season rather than considering forecast lead alone.

Predictability also differs among NASH quadrants. During the first predicted summer, the NW quadrant is among the most successfully predicted ridge configurations, whereas the NE quadrant exhibits comparatively lower predictability. Previous unini-

tialized climate-model studies have projected changes in the frequency of particular western ridge configurations, including increases in NW- and SW-type ridges (Li et al., 2019). Although the present analysis does not evaluate future changes in quadrant frequency, the differences in prediction skill among quadrants demonstrate that not all NASH configurations are equally predictable in an initialized forecast system. This motivates future work comparing initialized prediction skill with changes in NASH behavior simulated by uninitialized climate projections.

Overall, these results demonstrate measurable seasonal-to-multi-year predictability of NASH western ridge variability after systematic model bias is removed. At the same time, the remaining errors and strong dependence on season and quadrant show that predicting the large-scale circulation feature remains imperfect.

4.2 What Have We Learned About Precipitation Prediction Skill?

Compared with NASH western ridge position, SEUS precipitation is substantially more difficult to predict. The probabilistic verification metrics indicate that SMYLE contains some information about above- and below-average precipitation, but this information does not consistently translate into skill relative to climatology. The Brier Score (BS), Brier Skill Score (BSS), ROC AUC, reliability, and precipitation agreement diagnostics collectively show that the model's precipitation probabilities contain useful information in some seasons and leads, but forecast quality is strongly dependent on the metric.

The differences in these metrics are important and help determine the prediction skill. ROC AUC measures whether the forecast probabilities can discriminate between events and non-events, whereas the Brier score evaluates the overall probabilistic error, and the Brier skill score evaluates whether this error represents an improvement

relative to the CHIRPS climatology. A forecast could have discrimination while still exhibiting poor skill relative to climatology if the forecast probabilities are not predicted well. The reliability analysis similarly shows whether the magnitude of forecast probabilities corresponds to the observed event frequency. These diagnostics evaluate complementary aspects of precipitation forecast skill.

Conditioning the precipitation forecasts on NASH western ridge prediction provides additional insight into this relationship. Members that correctly predict the NASH quadrant generally perform better than members that predict the quadrant incorrectly for several precipitation diagnostics. However, selecting NASH-correct members does not consistently outperform the full ensemble. This is important because correctly predicting the large-scale NASH configuration provides useful information about precipitation, but NASH western ridge position alone is not sufficient to isolate the most skillful precipitation forecasts.

The spatial composites then reinforce this interpretation by showing how precipitation errors change depending on the direction and magnitude of the western ridge displacement. Forecasts where the ridge is displaced too far east or west produce different precipitation error structures, somewhat consistent with changes in the circulation associated with the position of the western ridge. However, small mean precipitation differences within some NASH position error categories don't necessarily mean high precipitation forecast skill. Composite averaging can reduce spatial errors when positive and negative precipitation anomalies occur among different cases. The probabilistic verification metrics are therefore necessary for determining forecast skill, while the composites provide a physical diagnostic of the circulation and precipitation structures associated with that skill.

4.3 Why Does Correct NASH Prediction Not Guarantee Correct Precipitation?

A central result of this study is that correctly predicting the NASH western ridge does not guarantee a correct precipitation forecast. Western ridge position represents only one component of the atmospheric state controlling SEUS precipitation. Two forecasts can place the western ridge within the same quadrant while still differing in exact ridge longitude and latitude, circulation strength, geopotential-height gradients, low-level winds, moisture transport, and regional atmospheric stability. Thus, quadrant correctness should be interpreted as successful prediction of the broad NASH configuration.

The circulation and precipitation composites illustrate a reproduction of the circulation. Even among forecasts classified into the same NASH skill category, differences remain between SMYLE and ERA5 circulation fields. Similarly, the mean western ridge locations calculated from individual cases do not necessarily fall exactly on the 1560-gpm contour of the composite field. Each western ridge location is diagnosed from the intersection of the 1560-gpm and zero-zonal-wind contours for that individual forecast. Averaging the resulting ridge locations and independently averaging the circulation fields are mathematically different. Spatial variability among cases smooths and shifts the composite contours, particularly for groups containing large variability in western ridge position.

The relationship between NASH position and precipitation also depends on the regional circulation associated with different ridge configurations. A northwestward ridge configuration can promote large-scale subsidence over portions of the SEUS, suppressing vertical motion and convection (Li et al., 2011). In contrast, southeastward

positioning of the western ridge can favor enhanced oceanic moisture transport into the SEUS (Sala et al., 2025). Therefore, errors in ridge longitude can alter the circulation and moisture pathways affecting regional precipitation even when the general NASH structure is represented.

At the same time, large-scale circulation is not the only source of SEUS precipitation variability. Land-atmosphere interactions, soil-moisture variability, atmospheric moisture availability, convection, and internal atmospheric variability can modify precipitation independently of the western ridge classification. These processes help explain why precipitation errors persist even when SMYLE correctly predicts the NASH quadrant and why NASH-conditioned forecasts do not consistently outperform the full ensemble. The NASH therefore provides a source of precipitation predictability, but it does not provide a complete predictor of SEUS precipitation.

4.4 Broader Implications

NASH and precipitation predictability have important implications for seasonal-to-multi-year climate prediction. For the SEUS, NASH western ridge predictions may provide useful context for forecasting the atmospheric conditions associated with precipitation variability, but uncertainty remains in translating circulation prediction skill into precipitation probabilities. This is relevant for several industries such as water-resource management, agriculture, and seasonal climate outlooks. Initialized predictions of NASH variability could contribute to forecast confidence when the signal is strong, particularly during seasons that exhibit greater predictability. However, the results presented here indicate that NASH information should be considered alongside other sources of predictability rather than used as the sole predictor of precipitation.

4.5 Limitations

Several limitations should be considered when interpreting these results. First, the analysis is based on a single initialized prediction system, CESM2-SMYLE. Unfortunately, it is not possible to determine whether the relationships are specific to SMYLE or are common features of initialized seasonal-to-multi-year prediction systems. This is because there are no other initialized models that could be used in this particular experiment.

Second, this study uses one definition of the NASH western ridge based on the intersection of the 1560-gpm geopotential-height contour and the zero-zonal- wind contour. Although this definition provides a consistent framework for tracking the western ridge, alternative definitions or geopotential-height thresholds could produce differences in diagnosed ridge position and prediction skill.

Third, the analysis uses monthly data. Monthly averaging is useful for evaluating seasonal-to-multi-year predictability but removes much of the synoptic and subseasonal variability that contributes to precipitation. Processes such as convection, moisture transport, and short-lived circulation anomalies may be missed as a result.

Fourth, the precipitation verification simplifies regional precipitation into above- and below-average events. This binary framework provides a clear probabilistic verification target but does not distinguish the magnitude of precipitation anomalies or explicitly evaluate extreme wet and dry events.

Finally, the bias correction applied in this study removes systematic mean-state errors from the model fields used to diagnose the NASH, but it does not alter the model physics or the dynamical evolution that produced those forecasts. Errors in moisture transport, convection, and land-atmosphere interactions therefore remain after bias correction.

4.6 Future Work

Future work should extend the analysis to daily data to determine how circulation variability on a shorter timescale contributes to the relationship between NASH position and precipitation. More frequent data would also make it possible to investigate whether correctly predicting the monthly-mean NASH state masks errors in the timing or persistence of individual circulation events.

Additional initialized prediction systems should also be evaluated as they become available to determine whether the relationships identified here are model-dependent. Comparison with uninitialized simulations would further help separate predictability arising from initialization from the model's ability to reproduce the behavior of the NASH. This comparison would also help determine whether future climate scenarios are causing the shift in the NASH and if uninitialized models would be a better representation for the prediction of the NASH position.

An especially important future study is to investigate the predictability of North Atlantic sea-surface temperature variability and its relationship with NASH western ridge prediction. Seasonal Atlantic SST variability, including variability associated with the Atlantic Multidecadal Oscillation, has been linked to changes in NASH intensity and position. Determining whether skillful SST predictions prime periods of enhanced NASH predictability could help identify the physical source of seasonal-to-multi-year NASH forecast skill.

Future precipitation analyses could also move beyond binary above- and below-average events to evaluate precipitation magnitude, extremes, and additional categorical thresholds. Finally, more statistical or machine-learning approaches could be explored as diagnostic tools for determining whether combining NASH position with SSTs, soil moisture, moisture transport, and other circulation variables improves pre-

cipitation prediction beyond that obtained from NASH western ridge position alone.

4.6.1 Summary and Conclusion

This study evaluated the seasonal-to-multi-year predictability of the NASH western ridge in CESM2-SMYLE and examined whether skillful prediction of this large-scale circulation feature improves prediction of SEUS precipitation. The primary conclusions are:

1. The SMYLE hindcasts exhibit measurable skill in predicting the location and seasonal variability of the NASH after correcting systematic biases, although skill varies strongly by season and quadrant.

2. NASH prediction errors are dominated by zonal (east–west) displacement, while meridional (north–south) errors remain comparatively small.

3. SEUS precipitation exhibits substantially more limited seasonal-to-multi-year probabilistic skill. Forecasts contain useful precipitation information in some cases, but they do not consistently outperform the climatological reference.

4. Correct prediction of the NASH quadrant is associated with improved precipitation forecast performance relative to incorrectly predicted NASH cases for several diagnostics, but NASH-correct members do not consistently outperform the full ensemble.

5. Therefore, skillful prediction of the NASH western ridge provides useful information about regional precipitation but is not sufficient to determine SEUS precipitation outcomes.

Reference List

Alexander, M. A., K. H. Kilbourne, and J. A. Nye, 2014: Climate variability during warm and cold phases of the atlantic multidecadal oscillation (amo) 1871–2008. *Journal of Marine Systems*, **133**, 14–26, https://doi.org/10.1016/j.jmarsys.2013.07.017.

Becker, E. J., E. H. Berbery, and R. W. Higgins, 2011: Modulation of cold-season u.s. daily precipitation by the madden–julian oscillation. *Journal of Climate*, https://doi.org/10.1175/2011JCLI4018.1.

Branstator, G., 2002: Circumglobal teleconnections, the jet stream waveguide, and the north atlantic oscillation. *Journal of Climate*, **15**, 1893–1910, https://doi.org/10.1175/1520-0442(2002)015⟨1893:CTTJSW⟩2.0.CO;2.

Chalise, D. R., A. Aiyyer, and A. Sankarasubramanian, 2021: Tropical cyclones' contribution to seasonal precipitation and streamflow over the southeastern and southcentral united states. *Geophysical Research Letters*, **48**, e2021GL094738, https://doi.org/10.1029/2021GL094738.

Cioni, G., and C. Hohenegger, 2017: Effect of soil moisture on diurnal convection and precipitation in large-eddy simulations. *Journal of Hydrometeorology*, https://doi.org/10.1175/JHM-D-16-0241.1.

Davis, R. E., B. P. Hayden, D. A. Gay, W. L. Phillips, and G. V. Jones, 1997: The north atlantic subtropical anticyclone. *Journal of Climate*.

Di Capua, G., J. Runge, R. V. Donner, B. van den Hurk, A. G. Turner, R. Vellore, R. Krishnan, and D. Coumou, 2020: Dominant patterns of interaction between the tropics and mid-latitudes in boreal summer: causal relationships and the role of timescales. *Weather and Climate Dynamics*, **1**, 519–539, https://doi.org/10.5194/wcd-1-519-2020.

Ek, M. B., and A. A. M. Holtslag, 2005: Evaluation of a land-surface scheme at cabauw. *Theoretical and Applied Climatology*, **80**, 213–227, https://doi.org/10.1007/s00704-004-0101-4.

Enfield, D. B., A. M. Mestas-Nuñez, and P. J. Trimble, 2001: The atlantic multidecadal oscillation and its relation to rainfall and river flows in the continental u.s. *Geophysical Research Letters*, **28**, 2077–2080, https://doi.org/10.1029/2000GL012745.

Ford, T. W., J. Steiner, B. Mason, and S. M. Quiring, 2023: Observation-driven characterization of soil moisture-precipitation interactions in the central united states. *Journal of Geophysical Research: Atmospheres*, **128**, e2022JD037 934, https://doi.org/10.1029/2022JD037934.

He, C., B. Wu, L. Zou, and T. Zhou, 2017: Responses of the summertime subtropical anticyclones to global warming. *Journal of Climate*, https://doi.org/10.1175/JCLI-D-16-0529.1.

Hoskins, B. J., 1996: On the existence and strength of the summer subtropical anticyclones. *Bulletin of the American Meteorological Society*, **77**, 1287–1292.

Hu, Q., S. Feng, and R. J. Oglesby, 2011: Variations in north american summer precipitation driven by the atlantic multidecadal oscillation. *Journal of Climate*, https://doi.org/10.1175/2011JCLI4060.1.

Kerr, R. A., 2000: A north atlantic climate pacemaker for the centuries. *Science*, **288**, 1984–1985, https://doi.org/10.1126/science.288.5473.1984.

Li, L., W. Li, and A. P. Barros, 2013: Atmospheric moisture budget and its regulation of the summer precipitation variability over the southeastern united states. *Climate Dynamics*, **41 (3-4)**, 613–631, https://doi.org/10.1007/s00382-013-1697-9.

Li, L., W. Li, and Y. Kushnir, 2012a: Variation of north atlantic subtropical high western ridge and its implication to the southeastern us summer precipitation. *Climate Dynamics*, **39**, https://doi.org/10.1007/s00382-011-1214-y.

Li, W., L. Li, R. Fu, Y. Deng, and H. Wang, 2011: Changes to the north atlantic subtropical high and its role in the intensification of summer rainfall variability in the southeastern united states. *Journal of Climate*, https://doi.org/10.1175/2010JCLI3829.1.

Li, W., L. Li, M. Ting, and Y. Liu, 2012b: Intensification of northern hemisphere subtropical highs in a warming climate. *Nature Geoscience*, **5 (11)**, 830–834, https://doi.org/10.1038/ngeo1590.

Li, W., T. Zou, L. Li, Y. Deng, V. T. Sun, Q. Zhang, J. B. Layton, and S. Setoguchi, 2019: Impacts of the north atlantic subtropical high on interannual variation of summertime heat stress over the conterminous united states. *Climate Dynamics*, **53**, 3345–3359, https://doi.org/10.1007/s00382-019-04708-1.

Liu, Y., and Coauthors, 2025: Basin-wide and coastal modes of north tropical atlantic variability have distinct impacts on hurricanes. *Communications Earth & Environ-*

ment, **6**, 549, https://doi.org/10.1038/s43247-025-02529-1.

Manthos, Z. H., K. V. Pegion, P. A. Dirmeyer, and C. Stan, 2022: The relationship between surface weather over north america and the mid-latitude seasonal oscillation. *Dynamics of Atmospheres and Oceans*, **99**, 101 314, https://doi.org/10.1016/j.dynatmoce.2022.101314.

Misra, V., A. Bhardwaj, and A. Mishra, 2018: Characterizing the rainy season of peninsular florida. *Climate Dynamics*, **51**, 2157–2167, https://doi.org/10.1007/s00382-017-4005-2.

Nigam, S., B. Guan, and A. Ruiz-Barradas, 2011: Key role of the atlantic multidecadal oscillation in 20th century drought and wet periods over the great plains. *Geophysical Research Letters*, **38**, https://doi.org/10.1029/2011GL048650.

Pegion, K., E. J. Becker, and B. P. Kirtman, 2022: Understanding predictability of daily southeast u.s. precipitation using explainable machine learning. *Journal of Climate*.

Rodwell, M. J., and B. J. Hoskins, 2001: Subtropical anticyclones and summer monsoons. *Journal of Climate*, **14**, 3192–3211, https://doi.org/10.1175/1520-0442(2001)014⟨3192:SAASM⟩2.0.CO;2.

Sala, C. M., E. Zorzetto, and L. Li, 2025: The contrasting roles of land and oceanic moisture contributions to summer rainfall over the southeastern united states. *Journal of Geophysical Research: Atmospheres*, **130 (3)**, e2024JD042 039, https://doi.org/10.1029/2024JD042039.

Schmidt, D. F., and K. M. Grise, 2019: Impacts of subtropical highs on summertime precipitation in north america. *Journal of Geophysical Research: Atmospheres*, **124**, 11 188–11 204, https://doi.org/10.1029/2019JD031282.

Schubert, S., H. Wang, and M. Suarez, 2011: Warm season subseasonal variability and climate extremes in the northern hemisphere: The role of stationary rossby waves. *Journal of Climate*, **24**, 4773–4792, https://doi.org/10.1175/JCLI-D-10-05035.1.

Schubert, S., and Coauthors, 2009: A u.s. clivar project to assess and compare the responses of global climate models to drought-related sst forcing patterns. *Journal of Climate*, https://doi.org/10.1175/2009JCLI3060.1.

Smith, E. T., and S. C. Sheridan, 2022: The relationship between teleconnections, surface temperature, and cold air outbreaks. *International Journal of Climatology*, **42**, 1531–1543, https://doi.org/10.1002/joc.7318.

Song, F., L. R. Leung, J. Lu, and L. Dong, 2018: Future changes in seasonality of the north pacific and north atlantic subtropical highs. *Geophysical Research Letters*, **45**, 11 959–11 968, https://doi.org/10.1029/2018GL079940.

Wang, H., R. Fu, A. Kumar, and W. Li, 2010: Intensification of summer rainfall variability in the southeastern united states during recent decades. *Journal of Hydrometeorology*, https://doi.org/10.1175/2010JHM1229.1.

Wei, W., W. Li, Y. Deng, and S. Yang, 2019: Intraseasonal variation of the summer rainfall over the southeastern united states. *Climate Dynamics*, **53**, 1171–1183, https://doi.org/10.1007/s00382-018-4345-6.

Xu, J., Y. Wang, and Z. M. Tan, 2016: The relationship between sea surface temperature and maximum intensification rate of tropical cyclones in the north atlantic. *Journal of the Atmospheric Sciences*, https://doi.org/10.1175/JAS-D-16-0164.1.

Zhang, W., B. Kirtman, L. Siqueira, B. Xiang, J. Infanti, and N. Perlin, 2022: Decadal variability of southeast us rainfall in an eddying global coupled model. *Geophysical Research Letters*, **49**, e2021GL096 709, https://doi.org/10.1029/2021GL096709.

Zhou, W., L. R. Leung, F. Song, and J. Lu, 2021: Future changes in the great plains low-level jet governed by seasonally dependent pattern changes in the north atlantic subtropical high. *Geophysical Research Letters*, **48**, e2020GL090 356, https://doi.org/10.1029/2020GL090356.

Zorzetto, E., and L. Li, 2021: Impacts of the north atlantic subtropical high on daily summer precipitation over the conterminous united states. *Journal of Hydrometeorology*, https://doi.org/10.1175/JHM-D-20-0242.1.